

## **A novel desorption technique for improved sensitivity in sampling for gases**

### **PI**

**Claudiu T. Lungu, Ph.D.**

Associate Professor  
Department of Environmental Health Sciences  
School of Public Health

University of Alabama at Birmingham  
1720 2nd Ave. South,  
Birmingham, AL 35294  
Phone: 205-934-2072; Fax: 205-975-6341  
[clungu@uab.edu](mailto:clungu@uab.edu)

### **Co-I**

**Evan Floyd, Ph.D.**

Assistant Professor  
Department of Occupational and Environmental Health  
College of Public Health  
University of Oklahoma Health Science Center  
801 Northeast 13th Street, Room 419  
Post Office Box 26901  
Oklahoma City, Oklahoma 73126-0901

### **Co-I**

**Andrei Stanishevsky, Ph.D.**

Associate Professor  
Department of Physics  
College of Arts and Sciences  
University of Alabama at Birmingham  
1720 2nd Ave. South,  
Birmingham, AL 35294

Grant number: **NIOSH/CDC – 1 R21 OH010373**

Start date: September 18, 2013

End date: August 30, 2015

November 26, 2015

## Table of Contents

Title page	1
Table of contents	2
List of terms and abbreviation	3
Abstract	4
Final Progress Report Section 1	6
Significant Findings	6
Translation of Findings	6
Outcomes/ Impact	7
Final Progress Report Section 2	8
Scientific report	8
Introduction	8
Adsorption and Single Walled Carbon Nanotubes	13
Photothermal Desorption	19
Reference	23
Background	27
Methods	30
Fabrication of SWNTs substrates	30
Fabrication of Chemical Vapor Deposition (CVD) buckypapers	30
First attempts for the fabrication of Arc Discharge (AC) buckypapers	31
Fabrication and characterization of SWNTs obtained through arc discharge (AD) and high-pressure carbon monoxide (HiPco) synthesis	33
Fabrication of CSP substrates through Hydrothermal Carbonization (HTC)	46
Co-Investigator's final report	50
List of publication	55

## List of Terms and Abbreviations

AC	Activated carbon
AD	Arc discharge
BET	Brunauer, Emmett, and Teller
BP	Buckypapers
CNT	Carbon nanotubes
CSP	Carbonaceous spherical particles
CVD	Chemical vapor deposition
DAIC	Diffusive based VOC adsorption isotherm chamber
GC	Gas chromatography
HiPco	High-pressure carbon monoxide
HTC	Hydrothermal carbonization
PTD	Photothermal desorption
PTFE	Polytetrafluoroethylene
SWCT	Single walled carbon nanotubes
VOC	Volatile organic compounds

## Abstract

### **A novel desorption technique for improved sensitivity in sampling for gases**

PI: Claudiu T. Lungu, Ph.D.  
Associate Professor  
Department of Environmental Health Sciences  
School of Public Health  
University of Alabama at Birmingham  
1720 2nd Ave. South,  
Birmingham, AL 35294  
Phone: 205-934-2072; Fax: 205-975-6341  
[clungu@uab.edu](mailto:clungu@uab.edu)

Millions of workers are occupationally exposed to volatile organic compounds (VOC) annually, air sampling being the most reliable method to assess their exposure; reducing time to knowledge, while maintaining adequate sensitivity and affordability is a constant struggle. Sorbent sampling is the preferred technique for VOC exposure assessment. Chemical desorption of sorbents is the most common desorption technique, but sensitivity is limited due to small injection fraction. Thermal desorption has excellent sensitivity, but provides only one analysis per sample and is cost prohibitive. We demonstrated a desorption technique that bridges the sensitivity gap between chemical desorption and thermal desorption techniques. We demonstrated that carbonaceous sorbents irradiated with high intensity light can be used to release enough analyte to be directly analyzed by gas chromatography or other analytical methods. Granular Activated Carbon (GAC) is the gold standard for volatile organic compound (VOC) sampling, but recently other carbonaceous porous materials like Single Walled Carbon Nanotubes (SWNT) and porous materials fabricated using Hydrothermal Carbonization (HTC) process have shown comparable adsorption and desorption attributes. Recent studies showed that SWNT efficiently absorb visible light and transform it in heat hinting that irradiation of samples loaded with vapors through air sampling could be desorbed by light irradiation. This will significantly simplify the current analytical methods and will increase sensitivity of analysis.

We fabricated several different matrix SWNT substrates based on Chemical Vapor Deposition (CVD), Arc Discharged (AC) and High Pressure Carbon Monoxide

(HiPco) synthesis techniques. We also fabricated high surface area carbonaceous spherical particles (CSP) from glucose precursors using Hydrothermal Carbonization (HTC). We characterized their physical and adsorption properties and for some of these substrates we quantified the percentage of analyte released when the loaded substrate was irradiated by various intensities of visible light. For most of the materials we fabricated we demonstrated that they can adsorb significant amount of toluene, used as a reference VOC and when irradiated with visible light a significant percentage of the analyte gets released to be detected by a field grade photo thermal detector (PID). For some of the proposed material configurations we did not succeed yet to produce self-supporting sorbent substrates to be re-used in passive samplers, because of the particular morphology of the materials. However, we were exploring innovative ways to fabricate and test carbonaceous porous materials from inexpensive precursors such as starch, glucose and other naturally occurring materials. We propose that further research to focus in this direction as well as in the making of a prototype sampler using the photothermal desorption technique.

## Final Progress Report Section 1

### Significant Findings

The scope of the research carried out in this project was to demonstrate a new air sampling and analysis concept in which volatile organic compounds (VOCs) are collected into a porous substrate and desorbed by irradiation with visible light. We demonstrated this novel analytical technique called **photothermal desorption** (PTD) which can improve the sensitivity of the analysis of passive samplers and help shorten the current exposure assessment procedure to improve workers' protection by faster turn-around-time for analytical results. Our finding showed that single walled carbon nanotubes (SWNT) obtained from various synthesis methods and fabricated into a thin layer (buckypaper) have high surface area and potentially can be used as sorbents for VOC sampling. We also showed that passive air samplers made with this SWNT substrate (felt) have similar characteristics for sampling toluene vapors as the 3M® OVM, one of the industry standard sampler. Additionally, we obtained through hydrothermal carbonization (HTC) high surface area carbonaceous spherical particles (CSP) using glucose as a precursor, which could be a less expensive alternative for sorbents used for VOC sampling.

### Translation of Findings

Occupational exposure assessment to VOCs commonly involves active or passive sampling using activated carbon (AC) sorbent, followed by chemical or thermal desorption. Chemical extraction accompanies gas chromatography (GC) analysis while thermal desorption is performed in a dedicated GC system. Passive sampling of volatile organic (VOCs) followed by laboratory analysis either through chemical or thermal extraction has been accepted in the workplace because of the convenience and cost effectiveness and wearer acceptability of passive sampler over active sampling devices. However, passive samplers are generally limited in capability for very low exposure situations or short duration sampling because of their higher limit of detection caused by the relatively slow sampling rate driven by diffusion. Moreover, for industries seeking to

demonstrate regulatory compliance, the long time lag between collecting samples and getting results back and expensive laboratory analysis have been a burden. In PTD, a pulse of light thermally desorbs the analyte collected on a sorbent which releases VOC. VOC can be directly measured with a photo-ionization detector (PID) or directed to a gas chromatograph (GC) for detailed analysis.

## **Outcomes/Impact**

In this project we laid down the foundation for a novel sampling and analytical technique which could result in developing a passive VOC sampler with improved sensitivity and faster analysis compared with the current sampling/analysis methods.

This new technique will impact the way exposure assessment for VOC is conducted in a number of ways:

- a. Will allow direct field screening of air samples collected during a work shift
- b. Will increase the sensitivity of the passive sampling process by allowing the release and analysis of a larger amount of analyte at a time
- c. Will reduce the analysis time by eliminating the waiting time for the chemical desorption to occur
- d. Will allow repeated analysis of a collected sample by repeated irradiation of the sorbent substrate

Ultimately, the new technique we demonstrated will have more versatility for the laboratory and field use and will reduce the steps in the sampling and analysis process. It will be allowing for more samples to be collected and analyzed in the same time interval increasing the confidence of the exposure assessment process.

## Final Progress Report Section 2

### Scientific Report

#### Introduction

##### *Air Sampling*

Each year millions of tons of volatile organic compounds (VOCs) are released in to the atmosphere from anthropogenic sources domestically and globally<sup>1-3</sup>. Undoubtedly a portion of these emissions result in occupational exposure to VOCs. Occupational exposure limits have been established by consensus and regulatory organizations based on health risks and technological limitations. Compliance with consensus standards such Threshold Limit Values (TLV) developed by the American Conference of Governmental Industrial Hygienists' (ACGIH) or Recommended Exposure Limits (REL) developed by the National Institute of Occupational Safety and Health (NIOSH) are voluntary, but compliance with regulatory standards such as Permissible Exposure Limits (PEL) established by the Occupational Health and Safety Administration (OSHA) are not. TLVs and RELs are health based limits that have been derived from risk assessments using epidemiological data and laboratory animal trials. These values have been set such that a given risk of negative health effects are not reasonably expected to occur in a small proportion of the population. PELs were established by OSHA in 1971 and were simply an adoption of existing consensus standards. As time has passes, updating the PELs to coincide with health based standard such as the TLV and REL has lagged and PELs tend to be less protective than TLVs and RELs.

To assess a workers occupational exposure there are two approaches; personal sampling and area sampling. Both techniques attempt to estimate the worker's exposure by measuring the concentration of contaminants in a representative air sample. Area sampling is conducted at a fixed location near the employee and attempts to collect a representative sample of the air in the same area as the employee. The representativeness of area samples depends on many factors including air flow patterns, homogeneity of the contaminant, proximity of the sampler to emission sources, proximity of the sampler to the worker, and worker mobility. Personal sampling attempts to collect a representative air sample from the worker's breathing zone (25 - 30 cm radius of the nose and mouth). The sampler is attached to the employee being monitored and is much closer to the local environment that the worker breathed during the work shift than are area samples. If the exposure environment changed due to worker mobility or process

changes this is directly reflected by the personal sample. For these reasons and more, personal sampling is the preferred approach.

Standard sampling and analysis methods have been developed for the assessment of occupational exposure to VOCs are capable of demonstrating both legal compliance and healthful protection of workers. These methods use a wide variety of sampling and analysis techniques. Sampling techniques include active sorbent sampling, passive sorbent sampling, whole air sampling and direct reading instrumentation. Analysis techniques include chemical desorption and thermal desorption of sorbents and dilution or pressurization of whole air samples with high purity inert gas for direct analysis by GC and/or GC-Mass Spectrometer. Each of these techniques has advantages and disadvantages some of which will be explored in the following paragraphs.

#### *Active Sorbent Sampling*

VOC Occupational exposure assessment samples have traditionally been collected by active sampling with a pump, sample line and charcoal sorbent tube. This technique has been used for decades, is robust and considered the gold standard for VOC exposure assessment. Fully validated methods exist for all of the chemical classes of VOC and sorbents have been developed that provide better affinities for some of the hard to measure polar solvents like alcohols and ketones. Several institutions and manufacturers have developed multi bed sorbent tubes that use different sorbents with different adsorption properties to collect the variety of potential VOC vapors<sup>4-7</sup>.

When using active sampling, the pump must be calibrated with a representative sampler in place before and after the exposure assessment and should not vary more than 5% from start to finish. After the representative air sample has been collected it must be stored in an appropriate location and transported to the lab for analysis. Sorbent samples are convenient because they pre-concentrate the VOCs from out of the air onto a small compact tube that can be easily stored and shipped. Analysis of active sorbent samples is performed by chemical desorption (solvent extraction) or thermal desorption. Chemical desorption is simply extraction of the sorbent by displacement and dissolution of the analyte from the sorbent into a solvent such as carbon disulfide (CS<sub>2</sub>) or methylene chloride (MeCl). Chemical desorption must use a solvent that demonstrates good desorption efficiency for the analyte(s) of interest. This process is somewhat time-consuming and tedious due to the manual removal of the sorbent from the glass sample tube and transfer into extraction vials, but it is simple and familiar to many bench

chemists. Typically, 100 mg of sorbent are extracted in 1 mL of solvent and 1  $\mu$ L injected into the Gas Chromatograph (GC) to quantify the VOCs collected during sampling. This results in approximately 1,000 times dilution of the collected sample and limits the sensitivity of the assessment.

Liquid injections into the GC are limited to a few micro-liters because of solvent expansion from the liquid to vapor phase. If too much solvent is injected into the inlet, the solvent expansion will overwhelm the inlet capacity, contaminate upstream system components causing sample carry over for many samples and cause poor chromatography such as peak fronting. Due to this sample introduction limitation, chemical desorption has inherently limited sensitivity.

Since such a small volume of sample is used for analysis, many analyses can be performed per extraction, but not as many as one might think. When preparing a sample for analysis on the GC the liquid level in the vial has to be above the mid-point of the vial otherwise the syringe needle will not pull any sample. GC vials are typically 1.5 mL volume but using vial inserts this can be reduced to 75 - 300  $\mu$ L effective volume. Once a GC vial septa is pierced it begins to evaporate. Typically the solvent preferentially evaporates over the analytes which results in an increase in analyte and internal standard concentration. Unless a GC vial is re-capped shortly after piercing, subsequent analyses will have higher results than original measured; this is correctable using internal standards but common practice is to re-vial a sample if secondary analysis is needed.

Depending on the volume of the GC vial inserts chosen, 3-10 re-vialings can be reasonably expected with chemical desorption.

Thermal desorption is the other desorption technique available for sorbent analysis. Simply put, heat is applied to the sorbent and analytes are back-flushed off of the sorbent onto a focusing trap. Depending on the analytes of interest and the sorbent that was used to collect the analytes, primary desorption times may range from 2-10 minutes, which eliminates preparation time but adds to instrument run-time. The focusing trap re-collects the desorbed sample on a cryogenically cooled segment of deactivated capillary column, a small diameter low mass sorbent tube or a cryogenically cooled sorbent trap. After the sample is completely desorbed, the focusing trap is rapidly heated (up to 100 $^{\circ}$ C/ sec) to release the sample over a short window of time. This second desorption is considered the injection into the GC. It is very important for the injection from the focusing trap to occur quickly, if the trap heats slowly then compounds will desorb at different rates and to varying degrees until the trap temperature gets above the critical

desorption temperature for all analytes and peak broadening will result. Peak broadening results in difficulty resolving similar compounds because more separation is necessary to attain the same degree of resolution as with sharper peaks. Analysis by thermal desorption requires no lab preparation and the samplers are re-usable many times. Historically, thermal desorption has been a one shot analysis; the whole sample is injected into the GC. Because of this thermal desorption has fantastic sensitivity and can be a good alternative to chemical desorption when sensitivity is a limitation. However, injecting the entire sample into the GC means that only one analysis is possible per sample and duplicate field samples must be collected which is unpopular with monitored workers.

Recently thermal desorption systems have been developed that split the desorption flow and recollect a programmable portion of the desorbed sample<sup>8</sup>. Initially these units were very expensive, but have started to come down in cost as second generation systems are developed and competitors enter the market. Their reliability has improved but they are still required by standard methods such as EPA TO-17 to continually verify a host of potential problems. Some of these quality checks include verifying gas tight sorbent tube, verifying gas tight seal between sorbent tube and desorption system, purge of air prior to desorbing sample and ensuring an inert flow path in the desorption system plumbing and transfer lines. These units have complex plumbing, switching valves, electric or cryogenic gas cold traps and multiple high temperature connections. Complying with the quality control checks may be simple when the system is new and uncontaminated by “dirty” samples with reactive and “sticky” chemicals, but verifying an inert flow path becomes difficult as a system ages.

### *Diffusive Sampling*

In the 1980's diffusive samplers were developed that do not require a pump to sample VOCs from the air. Diffusive samplers rely on chemical diffusivity and concentration gradients to sample VOCs in air. A small sorbent bed of fixed geometry is contained inside a diffusive cell. The diffusive cell has a porous membrane on one end and the sorbent bed on the other end. As vapors cross the membrane they migrate toward the sorbent bed based on concentration gradient. When the VOC touches the sorbent it is trapped by the sorbent through adsorption in micropores. The sampling rate depends on the sorbent cross sectional area, the diffusive path length and the chemical diffusivity of the particular vapor (figure 1). This sampling rate can be estimated with the following equation.

$$(1) S = \frac{KA}{L}$$

where:

S = sampling rate (cm<sup>3</sup>/min)

K = diffusion coefficient (cm<sup>2</sup>/min)

A = cross sectional area of sorbent (cm<sup>2</sup>)

L = diffusive path length (cm)

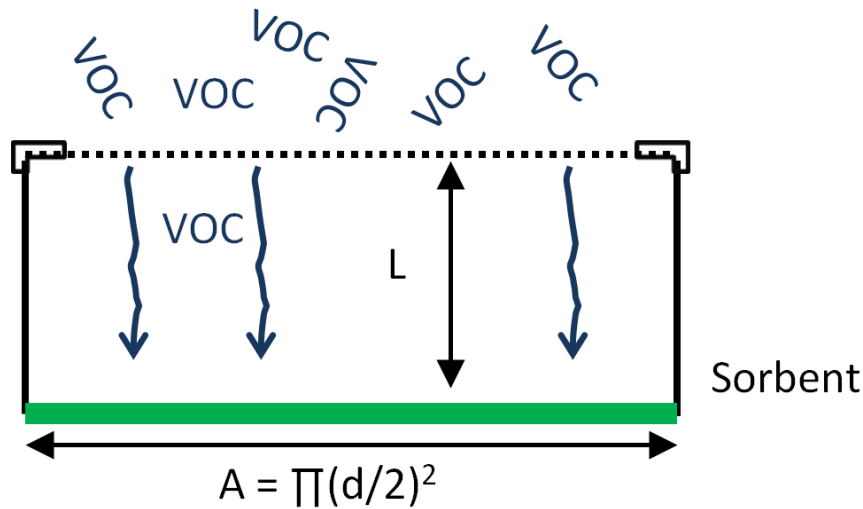


Figure 1: Schematic of a diffusive sampler

There is also a radial type diffusive sampler that operates on the same principles but with different geometric orientation.

While diffusive sampling eliminates the need for a sampling pump and tube, a moderate air velocity (~10 cm/ sec) across the face of the sampler is required in order to ensure a constant sampling rate. In active sampling, the sampling rate is the same for all compounds and is determined by the pump flow rate. For most methods sampling rates are between 10-200 mL/ min. Diffusive sampling rates are unique for each chemical and typically range between 10 - 40 mL/ min. In a situation where sensitivity is a limitation, sampling rates can be increased up to 200 mL/ min with active sampling but not for diffusive sampling. Therefore diffusive sampling

collects approximately one order of magnitude less sample than active sampling methods at the maximum sampling rate.

Analysis of diffusive sorbent samples is analogous to active sorbent samplers having chemical and thermal desorption options. In chemical desorption a greater volume of solvent is often times used due to the greater sorbent mass or volume needed to fully cover the sorbent with extraction solvent. These methods often call for increased injection volumes to make up for the lower sample concentration. Thermal desorption of most diffusive samplers requires transferring the sorbent from the sampler body to a thermal desorption tube, a step not necessary with active sorbent sampling with thermal desorption tubes.

## **Adsorption and Single Walled Carbon Nanotubes**

Although many sophisticated techniques exist for VOC measurement and exposure assessment, sorbent based sampling with chemical desorption remains the most common and trusted system for determining occupational VOC exposures. Diffusive sampling is popular with hygienists because of the light weight unobtrusive sampler, but low concentration and/ or short exposures need a larger sample volume to increase the mass collected, to lower the assessment sensitivity; this is not possible with diffusive samplers. Therefore, Industrial Hygienists gravitate toward active sorbent sampling for short term, low concentration assessment and diffusive sampling for long term assessments.

Adsorption of a molecule to a sorbent is governed by weak molecular forces, surface area and pore size. Weak molecular forces define the maximum analyte-sorbent interaction. Surface area influences adsorption rate and capacity with larger surface areas resulting in increased interaction between the analyte and sorbent. Pore size (pore diameter) affects the efficiency of the analyte-sorbent interaction<sup>9,10</sup>. When the pore size is approximately the same as analyte size, the interaction between the pore surface and the analyte approaches the potential of the weak molecular forces<sup>11,12</sup>. The pore provides a three dimensional field that acts on all surfaces of the analyte simultaneously<sup>9,13</sup>. As the pore size increases, pore walls become flatter and more distant. Analyte stabilization from the opposing walls becomes less affective and the analyte-sorbent interaction tends towards a two dimensional interaction on only one side of the molecule<sup>9,11-19</sup>.

For small organic molecules such as VOCs, small pores are more effective than large pores and high surface area is predictive of adsorption capacity. The traditional active sorbent sampler for

VOCs is constructed from granular activated carbon (AC) derived from coconut shells packed inside a glass tube. For polar VOCs such as light alcohols and ketones pore size and surface area are less predictive of adsorption capacity and collection efficiency than analyte-sorbent interaction. For these compounds, sorbents such as silica gel, Anasorb 747 and carbon molecular sieve are more effective than coconut shell activated carbon. Within thermal desorption, specialized sorbents have been engineered from graphitized carbons, polymeric beads and molecular sieves. In recent years other materials with high surface area such as activated carbon fibers and carbon nanotubes have been tested as organic vapor adsorbers with encouraging success<sup>11, 15, 16, 20-23</sup>. The carbonaceous structure of activated carbon and carbon nanotubes implies Van der Waals forces are the predominating weak molecular interaction. Since adsorption is governed by analyte-sorbent interaction and pore geometry, chemical composition and size are critical. A chemical that cannot interact with the pore walls due to composition or size will have low adsorption affinity and capacity. Micropores (diameter less than 2 nm) are most suitable for VOC adsorption because the pore diameter is comparable to molecular size. For example, toluene is a mid-sized VOC and has a kinetic diameter of 6 Å (0.6 nm), when a toluene molecule enters a micropore it is affected by the Van der Waals forces of the entire pore surface. No matter which surface it adsorbs to, the field effect of the surrounding pore walls lower its potential and thereby lowering its vapor pressure greatly. When a toluene molecule enters a mesopore (2 - 50 nm), only the nearest pore walls affect its potential. As toluene approaches a pore wall, the surface is relatively flat and far away from the opposing wall. There is minimal field effect from the opposing and surrounding pore walls and adsorption is basically two dimensional. There will be lower adsorption capacity and analyte-sorbent affinity in mesopores due to geometric limitations.

AC has a pore size distribution heavily weighted toward the micropore range<sup>17, 24-26</sup> with some mesopores and even fewer macro pores. Single walled carbon nanotubes SWNT have similar pore size distributions as AC<sup>12, 19, 27-29</sup>. Figures 2 and 3 show nitrogen adsorption isotherms for AC obtained from SKC (AC-SKC), SWNT powder (SWNT-p) obtained from M.K. Nano, Activated Carbon powder (AC-p) obtained from Sigma, and SWNT felt (SWNT-f) fabricated in-house from the SWNT-powder. Each adsorption isotherm was conducted at 77K using a Micromeritics ASAP 2020 equipped with micropore pressure transducer and multiple probe gas manifold by our collaborator Dr. Karim Sapag in the Physics Department of the Universidad Nacional de San Luis, Argentina.

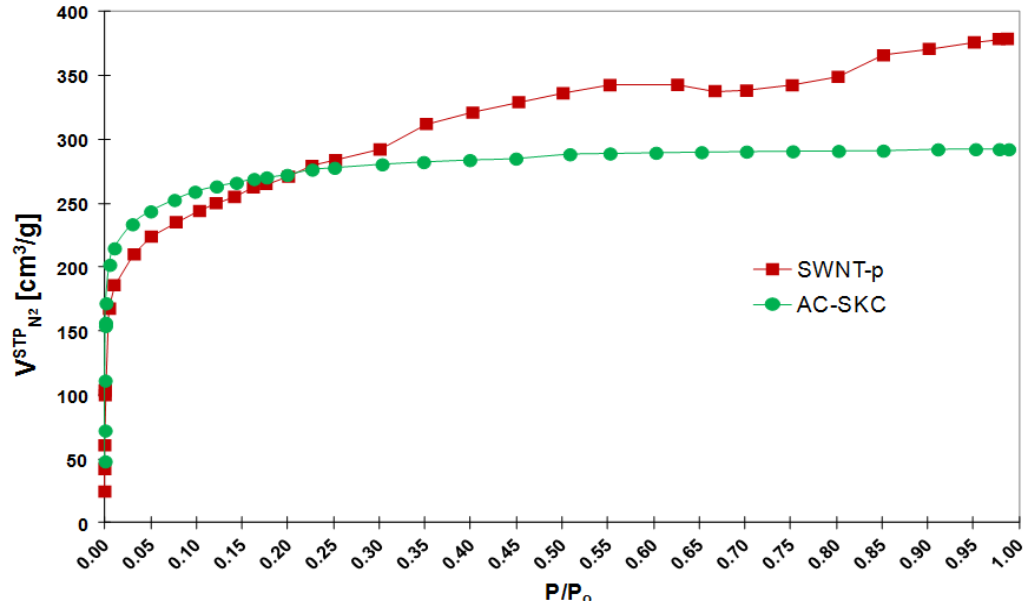


Figure 2: Nitrogen adsorption isotherm conducted with ASAP 2020 at 77K

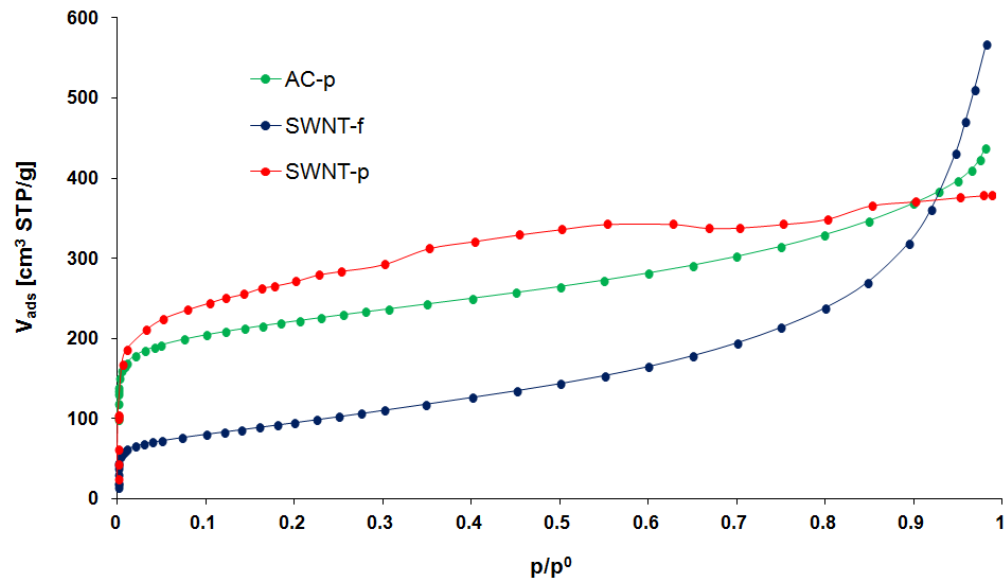


Figure 3: Nitrogen adsorption isotherm conducted with ASAP 2020 at 77K

From the nitrogen adsorption isotherm, a pore size distribution was calculated for each material using density functional theory. Figures 4 and 5 show the pore size distributions of the same materials shown in figures 2 and 3.

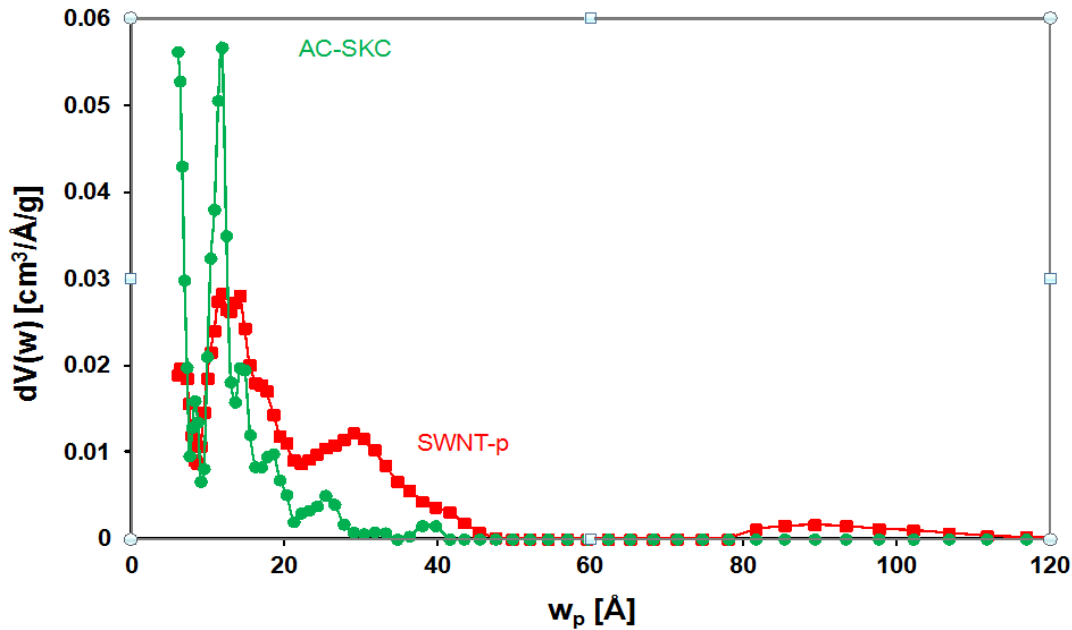


Figure 4: Pore size distribution of AC-SKC and SWNT-p derived from the N<sub>2</sub> adsorption isotherms using density functional theory.

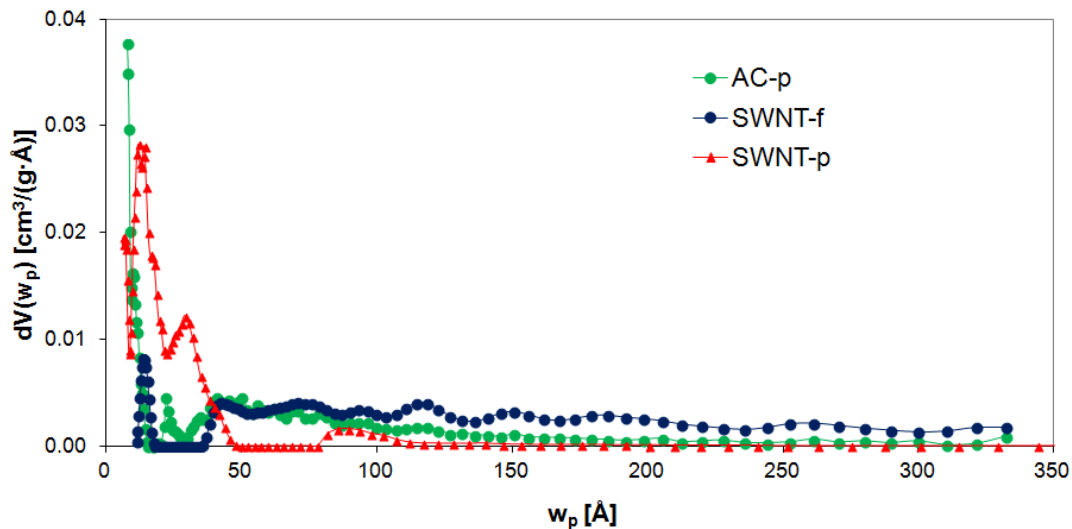


Figure 5: Pore size distribution of AC-p and SWNT-f derived from the N<sub>2</sub> adsorption isotherms using density functional theory.

In this preliminary study the concept of photothermal desorption to achieve partial desorption end points was performed using a continuous light source and commercially available materials (granular activated carbon purchased from SKC Inc. and single walled carbon nanotube powder purchased from M.K. Nano). Sorbents shown in figures 3 and 5 were used to demonstrate photothermal desorption via high powered camera flash. SWNT-p was processed into a felt

according to a technique described by Zheng et al.<sup>22</sup> which is similar in principle to many others<sup>30-34</sup>.

Additionally from the nitrogen adsorption isotherms we can determine the Brunauer Emmet and Teller (BET) surface area and porosity of each material. Table 1 shows a summary BET surface area, microporosity, and total porosity for each material evaluated.

	$S_{BET} [m^2/g]$	$-V_{\mu P} [cm^3/g]$	$V_{TP} [cm^3/g]$
<i>AC-SKC</i>	1030	0.41	0.45
<i>AC-p</i>	815	0.20	0.68
<i>SWNT-p</i>	980	0.39	0.59
<i>SWNT-f</i>	345	0.04	0.88

Table 1: BET surface area, microporosity and total porosity of the five sorbents evaluated by nitrogen porosymmetry.

In a micropore, the pore volume is filled layer by layer with the lowest energy positions occupied first until the remaining pore volume is filled and there is no difference between pore potential and environmental potential. BET surface area is generally preferred to the Langmuir surface area because it accounts for multi layer adsorption which is less likely to overestimate the true surface area. While the surface area of the two Activated Carbon samples are not identical, 1030 and 815 m<sup>2</sup>/g for AC-SKC and AC-p, respectively; they are both quite large and in the range expected for coconut shell activated carbons used for VOC sampling. The most notable difference in these two Activated Carbons is the microporosity, AC-SKC appears to have twice the microporosity of AC-p. This is evident in the pore size distribution plots, AC-SKC has a second large peak in the micropore region that is much larger than the second peak in AC-p. Also, the mesoporosity of the AC-p is much higher than that of AC-SKC. However, these differences did not greatly affect the toluene adsorption capacity.

SWNT-p when processed into SWNT-f was observed to have significantly lower surface area and microporosity, but significantly higher total porosity. This was an unexpected finding that indicates the highly disordered criss-crossing agglomerates provide additional microporosity that is not inherent to the tubular structure of SWNT. When SWNT-p was dispersed in toluene by sonication for 30 minutes or more some agglomerates would remain visible to the naked eye. If great care was taken to avoid pouring solution that had visible agglomeration, then a high quality felt was formed on the porous membrane filter. This high quality SWNT-felt had much

lower surface area, microporosity and toluene adsorption capacity than the source material. If little care was taken to avoid pouring suspensions with visible agglomerates, then a low quality felt was formed in which surface properties and adsorption capacities were slightly lower than the source material.

Scanning Electron Microscopy (SEM) imaging of the sorbents studied in chapters 3 and 4 (AC-p, SWNT-p and SWNT-f) was conducted at the UAB School of Engineering, Materials Science Department with the assistance of Dr. Robin Foley using an FEI Quanta FEG 650 microscope. Figures 6 and 7 are images taken at 20,000 V and 2.5 spot size at 100 and 5,000, and 100,000 magnification. At lower magnifications (figure 6) there is little distinguishable difference in the three substrates, except at 5,000x magnification AC-p appears to be jagged grains whereas SWNT-p and SWNT-f are rounded and smoother.

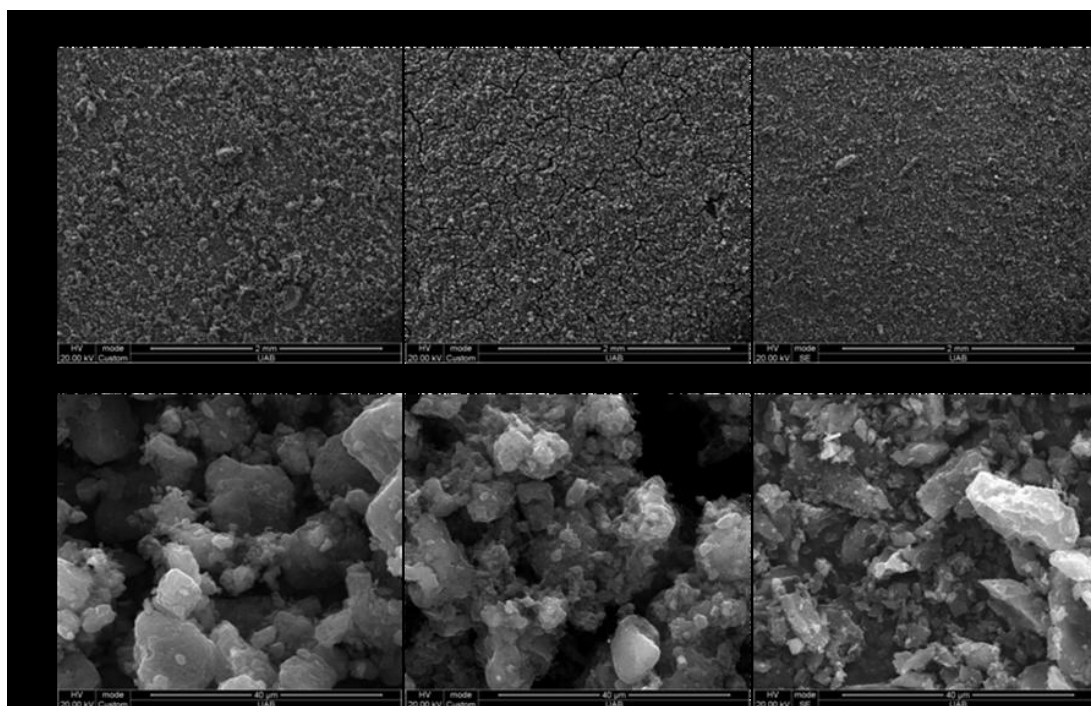


Figure 6: SEM images of SWNT-p, SWNT-f and ACP at 100x and 5,000x magnification.

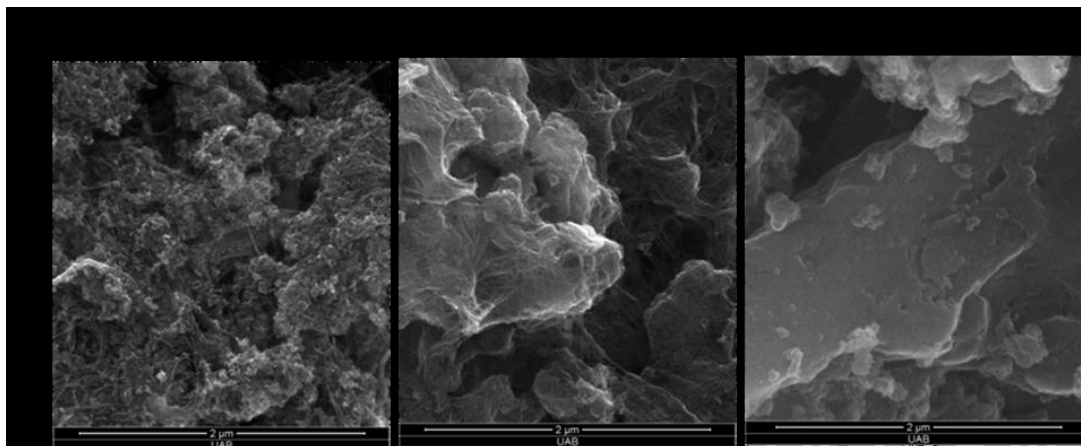


Figure 7: SEM images of SWNT-p, SWNT-f and ACP at 100,000x magnification.

At high magnification (100,000x) ropes and bundles of SWNT are visible and the surface morphology of the sorbents is easily differentiable. SWNT-p has significant surface texture that is formed by ropes of carbon nanotubes folded back on themselves and into the bulk, fibrosity is evident but almost all of the nanomaterial is in the form of large ropes and bundles tangled into large amorphous agglomerates, 4 - 10  $\mu\text{m}$  in diameter. In figure 6, at 5,000x magnification there is little visible difference between SWNT-p and SWNT-f. Both materials appear to be composed of small amorphous agglomerates of approximately equivalent diameter (4-10  $\mu\text{m}$ ), but at 100,000x magnification it becomes evident that the agglomerates in the SWNT-f sample have a webbing of carbon nanotube fibers overlaying them and connecting adjoining agglomerates. AC-p is very planar and jagged and easily discernible from either SWNT-p or SWNT-f sorbents.

Advances in SWNT synthesis techniques have increased the purity and surface area of “as-prepared” substrates<sup>35, 36</sup> and post synthesis purification techniques have yielded very pure SWNT with very high surface areas<sup>27, 28</sup>. With these advances, SWNTs are comparable to AC in surface area and microporosity and can be grown directly on precision micro components or formed into felts and aerogels if desired. As technology and production scale continue to increase, the economic difference between AC and SWNT narrows and adsorption applications are becoming more economically feasible.

## Photothermal Desorption

### *The Photothermal Effect*

Another interesting property of SWNT is their near black body absorption of UV-Vis electromagnetic radiation<sup>37-39</sup> and conversion into heat. This phenomenon has been observed

and applied in various fields of study ranging across bio-medical<sup>40-43</sup>, military<sup>44, 45</sup> and electronics<sup>46, 47</sup>. Ajayan, Bockrath and Tseng have demonstrated that a camera flash produces enough energy to heat SWNT fluff to the point of auto-oxidization and even ignition when irradiated in air<sup>48-50</sup>. Each of these researchers agree that as the matrix becomes denser and more interconnected the surface temperature is lower due to its conduction into the bulk of the material. In order for ignition to occur the matrix must be loose and fluffy with ample air between fibers and considerable iron catalyst residue from the synthesis process. The iron particles have a lower energy of activation for oxidation than that of C-C bonds and the light flash causes the residual iron catalysts to ignite which in turn ignites the carbon nanotubes<sup>50</sup>. As SWNT purity and density increase, the matrix becomes more resistant to ignition and oxidation because the heat load is dissipated from the surface where atmospheric oxygen is present.

An intentionally interconnected SWNT substrate such as SWNT felt, also known as bucky paper, can easily be fabricated and used to dissipate the heat from the light flash evenly throughout the matrix. This could be used as a technique to rapidly heat a sorbent sample and release a portion of the adsorbed VOCs. Traditional thermal desorption units heat the sorbent from the outside-in. A heating jacket surrounds the sorbent sampler and heat flows from the jacket to the sorbent tube body, to the sorbent. These systems have a relatively large thermal mass and cannot heat quickly and briefly; therefore, once sample desorption begins the whole sample must be desorbed from the original sorbent in order to achieve a reliable end point (zero remaining). In order to achieve a partial analysis of a thermally desorbed sample the desorption purge flow must be split and re-collected on another sorbent tube. A simpler approach to achieving partial analysis is to only desorb a fraction of the sample from the sorbent in the first place. Using light flash to rapidly heat a SWNT-felt sorbent could be used to desorb a portion of the sample while minimizing "sample bleed" due to slow thermal relaxation while retaining the balance of the sample on the original sorbent.

Using light energy to directly heat the sorbent reverses the flow of heat within the system; heat now flows from the sorbent to the desorption system. Since light absorption occurs on a quantum level this is a much faster process than conduction or radiative cooling. As soon as a photon strikes the sorbent its energy is absorbed and converted into heat in the form of molecular vibrations. This energy is transferred to the analyte and the desorption system through conduction and emission of small quantized packets of energy in the infra red region (radiative heat). Applying energy through a light flash allows a rapid heating cycle (milliseconds) followed by a much slower cooling cycle (few seconds). With this approach the sample can be

heated to 200°C for a few milliseconds and then returned to starting temperature within seconds, this is comparable if not superior to automated liquid injection.

A sorbent sampler specifically designed for use with photothermal desorption could be a modular sampling cartridge that can be used as a diffusive sampler and then placed directly in an irradiation chamber where light flash is applied and the desorbed analytes fed directly to a GC for analysis. Unlike thermal desorption, a focusing trap would not be necessary to re-collect the sample for a uniform injection into the GC because the desorption process is already so fast (<5 ms).

Simplification of the desorption process has the added benefit of reducing technician induced error such as sorbent loss during tube breaking and/ or transferring the sorbent for analysis and makes the process faster. Application of this technique is not limited to analytical laboratories; this could be developed into an attachment for portable direct reading field instruments such as PID, GC and GC/MS. Personal exposure assessment samples collected during a shift or task could be screened on-site for total VOC using a PID. Samples whose total VOC value is below any level of concern could be withheld from expensive lab analyses, while samples near or above potential levels of concern would be shipped to a lab for detailed analysis.

The main goal of this project was to demonstrate that photothermal desorption can be used to achieve reliable partial desorption of carbon based sorbent samples and that a highly interconnected thermally conductive sorbent such as SWNT-f would be most suitable for further investigation.

Two sorbents (AC-SKC and SWNT-p) are evaluated at various light powers and several desorption configurations. This study served several purposes; 1.) to demonstrate the feasibility of more sophisticated evaluations, 2.) to demonstrate the parity with traditional thermal desorption, 3.) to demonstrate reliability of a photothermal method 4.) to characterize boundaries for control parameters and experimental design. Samples were preloaded with toluene and irradiated with continuous light for several minutes, SWNT-p released significantly more toluene than AC-SKC.

### *Preliminary Study*

We determined the surface area of SWNT-p and granulated activated carbon samples using the Micromeritics ASAP 2020 in our research lab. The BET surface area was calculated from nitrogen adsorption at 77K and found to be 1033 m<sup>2</sup>/g and 880 m<sup>2</sup>/g, respectively. Prototype

samplers were constructed in a similar manner as traditional active sorbent samplers. SWNT powder was deposited inside 6 mm glass tube by dry pipetting SWNT powder into the 6 mm tube while under vacuum aspiration (Figure 9). The fabricated samplers were similar in construction to the SKC<sup>®</sup> 226-01 sampling tubes, however the resistance to flow was approximately 100 times greater in the SWNT sampler. Mixtures of toluene in air were prepared in a 100 liter Tedlar<sup>®</sup> bag at 5, 25, 50, 75 and 100 ppm. Triplicate samples were collected by drawing air at 30 mL/min using both the SWNT samplers and SKC<sup>®</sup> sampling tubes. All samples were extracted using the standard chemical desorption technique outlined in NIOSH analytical method 150157. On average, toluene recovery from the SWNT samples was significantly lower than that recovered from the SKC<sup>®</sup> samplers. Desorption efficiency studies showed near perfect recovery for both sorbents. Since back-up sections of activated carbon showed no breakthrough during active sampling for either sorbent, we concluded that analysis by chemical desorption of VOCs collected by active sampling not suitable.



Figure 9: Dry pipetting powdered SWNT into 6 mm sorbent tube bodies while under vacuum aspiration.

This could have been due to the much higher vacuum needed to pull 30 mL/ min through the SWNT-p sorbent bed. This lower pressure would shift the equilibrium towards desorption and could explain our results.

Zheng et al.<sup>22</sup> attempted a similar study and found “significant technical difficulties in fabricating active samplers from powdered SWNT, primarily the great resistance to flow and the risk of exposure to SWNT from fugitive nanotubes during material handling and experimentation” he also found that the temperature needed to desorb methyl ethyl ketone, toluene and DMMP from a SWNT substrates were well above the boiling point of each analyte and well above that

required to thermally desorb from the synthetic sorbent Tenax. An alternative approach to using powdered nanomaterials is to use bound nanomaterials such as felts and arrays. Zheng fabricated SWNT felt, cut the felt into strips, rolled the strips and packed them into a thermal desorption tube.

## REFERENCES

1. Singh, H. B.; Salstein, D. A. *Composition, Chemistry, and Climate of the Atmosphere. 2: Mean properties of the atmosphere*; 1994; p Medium: P; Size: 32 p.
2. Goldstein, A. H.; Galbally, I. E., *Environmental Science & Technology* 2007, 41 (5), 1514-1521.
3. USEPA The National Emissions Inventory.  
<http://www.epa.gov/ttn/chief/net/2008inventory.html>
4. Thermal Desorption Sorbent Tubes for Sub-ppb VOC Measurements. SKC Inc.:  
<http://www.skcinc.com/prod/226-356.asp>, 2013;
5. Industrial hygiene technical manual. U.S. Dept. of Labor, Occupational Safety and Health Administration: [Washington, D.C.?], pp 1 v. (loose-leaf).
6. Jeffress, C. N., OSHA technical manual. U.S. Dept. of Labor, Occupational Safety and Health Administration: Washington, D.C.,
7. Thermal Desorption Tubes - Versatile Air Sampling for a Wide Range of Applications:  
<http://www.restek.com/pdfs/EVFL1065.pdf>, 2008; Vol. EVFL 1065,
8. Unity Series 2 Thermal Desorber. Markes International, Ltd.,: [www.markes.com](http://www.markes.com), 2010;
9. Pan, B.; Xing, B., *Environmental Science & Technology* 2008, 42 (24), 9005-9013.
10. Allen, T., *Particle Size Measurement: Volume 2: Surface Area and Pore Size Determination*. Springer: 1996; Vol. 2,
11. Bosnick, K.; Ban, S.; Hiebert, W.; Shi, Z.; Huang, C.; Lister, R.; Mleczko, M., *Carbon* 2011, 49 (11), 3639-3644.
12. Eswaramoorthy, M.; Sen, R.; Rao, C. N. R., *Chemical Physics Letters* 1999, 304 (3-4), 207-210.
13. Ma, X.; Anand, D.; Zhang, X.; Talapatra, S., *The Journal of Physical Chemistry C* 2011, 115 (11), 4552-4557.
14. Crespo, D.; Yang, R. T., *Industrial & engineering chemistry research* 2006, 45 (16), 5524-5530.
15. Hussain, C. M.; Saridara, C.; Mitra, S., *Analyst* 2008, 133 (8), 1076-1082.

16. Balanay, J. A. G.; Crawford, S. A.; Lungu, C. T., *Journal of Occupational and Environmental Hygiene* 2011, 8 (10), 573-579.
17. Chiang, Y. C.; Chiang, P. C.; Huang, C. P., *Carbon* 2001, 39 (4), 523-534.
18. Hussain, C. M.; Saridara, C.; Mitra, S., *Analyst* 2009, 134 (9), 1928-1933.
19. Agnihotri, S.; Kim, P.; Zheng, Y.; Mota, J. P. B.; Yang, L., *Langmuir* 2008, 24 (11), 5746-5754.
20. Takada, S.; Nakai, T.; Fujita, W.; Thurakitserree, T.; Shiomi, J.; Maruyama, S.; Takagi, H.; Shuzo, M.; Delaunay, J. J.; Yamada, I. In *Evaluation of adsorption capacity of single-walled carbon nanotubes for application to micro gas preconcentrators*, *Sensors*, 2010 IEEE, 1-4 Nov. 2010; 2010; pp 2500-2503.
21. Takada, S.; Nakai, T.; Thurakitserree, T.; Shiomi, J.; Maruyama, S.; Takagi, H.; Shuzo, M.; Delaunay, J. J.; Yamada, I., *IEEJ Transactions on Sensors and Micromachines* 2010, 130 (6), 207-211.
22. Zheng, F.; Baldwin, D. L.; Fifield, L. S.; Anheier, N. C.; Aardahl, C. L.; Grate, J. W., *Analytical Chemistry* 2006, 78 (7), 2442-2446.
23. Saridara, C.; Mitra, S., *Analytical chemistry* 2005, 77 (21), 7094-7097.
24. Su, W.; Zhou, L.; Zhou, Y., *Chinese Journal of Chemical Engineering* 2006, 14 (2), 266-269.
25. El-Merraoui, M.; Aoshima, M.; Kaneko, K., *Langmuir* 2000, 16 (9), 4300-4304.
26. Dombrowski, R. J.; Hyduke, D. R.; Lastoskie, C. M., *Langmuir* 2000, 16 (11), 5041-5050.
27. Hu, Y. H.; Ruckenstein, E., *Industrial & Engineering Chemistry Research* 2004, 43 (3), 708-711.
28. Cinke, M.; Li, J.; Chen, B.; Cassell, A.; Delzeit, L.; Han, J.; Meyyappan, M., *Chemical Physics Letters* 2002, 365 (1-2), 69-74.
29. Murata, K.; Kaneko, K.; Kokai, F.; Takahashi, K.; Yudasaka, M.; Iijima, S., *Chemical Physics Letters* 2000, 331 (1), 14-20.
30. Hennrich, F.; Lebedkin, S.; Malik, S.; Tracy, J.; Barczewski, M.; Rosner, H.; Kappes, M., *Physical Chemistry Chemical Physics* 2002, 4 (11), 2273-2277.
31. Hilding, J.; Grulke, E. A.; George Zhang, Z.; Lockwood, F., *Journal of Dispersion Science and Technology* 2003, 24 (1), 1-41.
32. Wu, Z.; Chen, Z.; Du, X.; Logan, J. M.; Sippel, J.; Nikolou, M.; Kamaras, K.; Reynolds, J. R.; Tanner, D. B.; Hebard, A. F.; Rinzler, A. G., *Science* 2004, 305 (5688), 1273-1276.

33. Zhang, X.; Sreekumar, T. V.; Liu, T.; Kumar, S., *The Journal of Physical Chemistry B* 2004, 108 (42), 16435-16440.
34. Zhang, M.; Fang, S.; Zakhidov, A. A.; Lee, S. B.; Aliev, A. E.; Williams, C. D.; Atkinson, K. R.; Baughman, R. H., *Science* 2005, 309 (5738), 1215-1219.
35. Murakami, Y.; Chiashi, S.; Miyauchi, Y.; Maruyama, S. In *Direct Synthesis of Single-Walled Carbon Nanotubes on Silicon and Quartz Based Systems*, The International Symposium on Micro-Mechanical Engineering, 2003;
36. Maruyama, S.; Kojima, R.; Miyauchi, Y.; Chiashi, S.; Kohno, M., *Chemical Physics Letters* 2002, 360 (3-4), 229-234.
37. Mizuno, K.; Ishii, J.; Kishida, H.; Hayamizu, Y.; Yasuda, S.; Futaba, D. N.; Yumura, M.; Hata, K., *Proceedings of the National Academy of Sciences* 2009, 106 (15), 6044-6047.
38. Kataura, H.; Kumazawa, Y.; Maniwa, Y.; Umezumi, I.; Suzuki, S.; Ohtsuka, Y.; Achiba, Y., *Synthetic Metals* 1999, 103 (1-3), 2555-2558.
39. Tabakman, S. M.; Welsher, K.; Hong, G.; Dai, H., *The Journal of Physical Chemistry C* 2010, 114 (46), 19569-19575.
40. Moon, H. K.; Lee, S. H.; Choi, H. C., *Acs Nano* 2009, 3 (11), 3707-3713.
41. Burke, A.; Ding, X.; Singh, R.; Kraft, R. A.; Levi-Polyachenko, N.; Rylander, M. N.; Szot, C.; Buchanan, C.; Whitney, J.; Fisher, J., *Proceedings of the National Academy of Sciences* 2009, 106 (31), 12897-12902.
42. Chakravarty, P.; Marches, R.; Zimmerman, N. S.; Swafford, A. D.-E.; Bajaj, P.; Musselman, I. H.; Pantano, P.; Draper, R. K.; Vitetta, E. S., *Proceedings of the National Academy of Sciences* 2008, 105 (25), 8697-8702.
43. Robinson, J. T.; Welsher, K.; Tabakman, S. M.; Sherlock, S. P.; Wang, H.; Luong, R.; Dai, H., *Nano research* 2010, 3 (11), 779-793.
44. Malec, C. D.; Voelcker, N. H.; Shapter, J. G.; Ellis, A. V., *Materials Letters* 2010, 64 (22), 2517-2519.
45. Kang, B.; Dai, Y.; Chang, S.; Chen, D., *Carbon* 2008, 46 (6), 978-981.
46. Cote, L. J.; Cruz-Silva, R.; Huang, J., *Journal of the American Chemical Society* 2009, 131 (31), 11027-11032.
47. Snow, E. S.; Perkins, F. K.; Robinson, J. A., *Chemical Society Reviews* 2006, 35 (9), 790-798.
48. Ajayan, P.; Terrones, M.; De La Guardia, A.; Huc, V.; Grobert, N.; Wei, B.; Lezec, H.; Ramanath, G.; Ebbesen, T., *Science* 2002, 296 (5568), 705-705.

49. Bockrath, B.; Johnson, J. K.; Sholl, D. S.; Howard, B.; Matranga, C.; Shi, W.; Sorescu, D., *Science* 2002, 297 (5579), 192-193.

50. Tseng, S. H.; Tai, N. H.; Hsu, W. K.; Chen, L. J.; Wang, J. H.; Chiu, C. C.; Lee, C. Y.; Chou, L. J.; Leou, K. C., *Carbon* 2007, 45 (5), 958-964.

## Background

In the industrial hygiene field, granular activated carbon (GAC) is the gold standard for sampling volatile organic compounds (VOCs) from air. GAC is an effective adsorbent for organic vapors and some other gases because of its high surface area and porosity, and is widely used due to its ease of manufacturing and affordability. Chemical extraction from GAC dominates as the preferred desorption technique because it typically yields a robust sample that can be analyzed multiple times. However, when sampling toxic VOCs at low concentrations or measuring short term exposures, assessment is limited by the low analytical sensitivity of this technique.

Thermal desorption is an alternative extraction technique that facilitates higher analytical sensitivity by delivering more of the collected sample to the instrument. However, slow sample throughput, expensive dedicated equipment, and only one analysis per sample has limited the prevalence of this technique. There is a need for improved sampling methods that should be highly sensitive and provide a near instantaneous response to characterize exposure in the field. We propose here a novel system that could be as robust as chemical desorption with the enhanced sensitivity of thermal extraction. Recently, single walled carbon nanotubes (SWNT) have been demonstrated to have strong optical absorption in the UV-visible range,<sup>1,2</sup> effect not observed in GAC to the same magnitude. Exposure of a SWNT matrix to a high intensity light flash induces a sudden rise in temperature<sup>3,4</sup> (photo-thermal effect) causing combustion in some cases. SWNT have also been demonstrated as effective VOC adsorbents<sup>5,6,7,8,9</sup> being used in vapor preconcentrators<sup>7,8,10,11,12</sup>. Additionally, we obtained through hydrothermal carbonization (HTC) high surface area carbonaceous spherical particles (CSP) using glucose as a precursor, which could be a less expensive alternative for sorbents used for VOC sampling. We demonstrated that when the photo-thermal effect is used in conjunction with adsorptive properties, a new air sampling technique emerges with some significant advantages over the existent ones.

**For this project our hypothesis is that: SWNT and CSP based substrates can be used as sorbent sampling media for VOCs and thermally desorbed by irradiation with high intensity, visible spectrum light.**

To test the hypothesis the following specific aims were used:

**Aim 1: Fabricate SWNT and CSP substrates and characterize their adsorption properties**

**Aim 2: Measure the substrates' temperature response for various irradiation scenarios to determine the irradiation pattern that will yield the highest desorption rate from the substrates.**

**Aim 3: Characterize desorption from the microporous substrates using the most efficient irradiation patterns obtained in Aim 2.**

Most of the scientific report will focus on Aim 1 which has been expanded to fabricate and characterize a number buckypapers obtained from SWNT synthesized by various methods. This work resulted in a better estimate of the materials needed for the photothermal adsorption technique to be effective. We also made important steps in characterizing the BPs by developing and testing a diffusive based VOC adsorption isotherm chamber (DAIC) which will be used in further projects.

## References

1. K. Mizuno, A black body absorber from vertically aligned single-walled carbon nanotubes, *PNAS*, 106-15, 6044–6047 (2009)
2. H. Katarua, Optical Properties of Single-Walled Carbon Nanotubes, *Synthetic Metals*, 103, 2555-2558, (1999)
3. P. Ajayan, Carbon nanotubes in a flash – Ignition and reconstruction, *Science*, 296, 705 (2002)
4. S. Tseng, Ignition of carbon nanotubes using a photoflash, *Carbon*, 45, 958-964, (2007)
5. Z. Wu, Z. Chen, Transparent, Conductive Carbon Nanotube Films, *Science*, 305, 1273-1276 (2004)
6. F. Zheng, Single-walled carbon nanotube paper as a sorbent for organic vapor preconcentration, *Analytical Chemistry*, 78, 2442-2446 (2006)
7. S. Takada, Micro Gas Preconcentrator Made of a Film of Single-Walled Carbon Nanotubes, *IEEJ Transactinos on Sensors and Micromachines*, Vol 30 No 6, 207-211, (2010)

8. S. Takada, Evaluation of Adsorption Capacity of Single-Walled Carbon Nanotubes for Application to Micro Gas Preconcentrators, *IEEE Sensors*, (2010)
9. C. Saridara, Preconcentration of volatile organics on self-assembled, carbon nanotubes in a microtrap, *Anal. Chem*, 77, 1183-1187, (2005)
10. C. Hussain, Micropreconcentration units based on carbon nanotubes, *Anal Bioanal Chem*, 399, 75–89, (2011)
11. C. Hussain, C. Saridara, Microtrapping characteristics of single and multi-walled carbon nanotubes, *J. Chromatography*, 1185 (2), 161-166, (2008)
12. Y. Shih, Adsorption of selected volatile organic vapors on multiwall carbon nanotubes, *J. Hazard Matter*, 154, 21-28, (2008)

## Methods

### Fabrication of SWNTs substrates

Single walled carbon nanotubes (SWNTs) fabricated by different methods were purchased. These include chemical vapor deposition (CVD) SWNT suspended in n-methyl-2-pyrrolidone (NMP) (3 wt%, Nanoamor), arc discharge SWNT suspended in proprietary surfactants (NanoIntegris), and high pressure carbon monoxide (HiPco) SWNT powdered (NanoIntegris). Felts of CVD and arc discharge SWNTs have been fabricated and delaminated from a membrane filter to obtain buckypapers.

### Fabrication of Chemical Vapor Deposition (CVD) buckypapers

For the fabrication of a CVD SWNT felt, 800  $\mu\text{l}$  of SWNT solution was suspended in 800 ml of NMP and ultrasonicated for 30 minutes (31 mg SWNT/L). The SWNT solution was vacuum filtered through a polytetrafluoroethylene (PTFE) membrane filter (47 mm with 5  $\mu\text{m}$  pore, Millipore) and the felt was dried under vacuum and then in the oven for a minute to remove any residual NMP. Since NMP is viscous (1.7 cP at 20  $^{\circ}\text{C}$ ), the felt generated was swirled while slowly dried. NMP was thus diluted to the ratios of 5:5, 6:4, 7:3, and 8:2 as deionized (DI) water to NMP for suspending the SWNT solution. Samples were downscaled and concentrations of the solutions were about 25 mg SWNT/L. At 5:5 ratio, 7  $\mu\text{l}$  of SWNT solution was suspended in 4 ml of DI water and 4 ml of NMP, at 6:4 ratio 32  $\mu\text{l}$  of SWNT solution was suspended in 24 ml of DI water and 16 ml of NMP, and 32  $\mu\text{l}$  SWNT solution was suspended in 28 ml DI water and 12 ml NMP at 7:3 ratio. The solutions were then ultrasonicated for 30 minutes, and vacuum filtered (Figure 1.a, 1.b & 1.c). All felts were swirled at all of the ratios examined above.



Figure 1 CVD SWNT Felt from (a) 5:5 (water: NMP) Suspension (b) 4:6, and (c) 3:7

At 8:2 ratio, 32  $\mu$ l of SWNT solution was suspended in 32 ml DI water and 8 ml NMP, and the solution was ultrasonicated for 30 minutes and vacuum filtered with and without an aid of heating tape to help NMP evaporate (Figure 2.a & 2.b).



Figure 2 CVD SWNT Felt from 8:2 (water: NMP) Suspension (a) Naturally dried and (b) Dried under a heating tape

Since at the 2:8 ratio the felt was swirled the least and behaved better with the aid of a heating tape for drying, the SWNT solution concentration was increased to contain 1600  $\mu$ l suspended in 640 ml DI water and 160 ml NMP to make a buckypaper. 30 minutes of sonication and vacuum filtration were performed. After the filtration, the felt was dried with the help of a heating tape. The felt was swirled a little but easily delaminated from its filter membrane. The peeled buckypaper was flexible and it became flat between glasses for several hours (Figure 3.a & 3.b). As time had passed, however, the buckypaper shrank to half of its size. We decided to abandon the CVD synthesized SWNT route and to try making BP substrates using other synthesized methods for SWNTs .



Figure 3 CVD SWNT Buckypaper from 8:2 (water: NMP) Suspension (a) Front and (b) Back

### **First attempts for the fabrication of Arc Discharge (AC) buckypapers**

For the fabrication of an **arc discharge (AC)** SWNT felt, 200 ml of SWNT solution was mixed with 400 ml of acetone (125 mg SWNT/L) according to the company's instruction and suspended for about 18 hours. The solution was vacuum filtered through a PTFE membrane

filter, stabilized in vacuum for 15 minutes, and the felt was dried on a clean glass surface. The felt was then delaminated from its filter membrane to get a buckypaper and the buckypaper was pretty sturdy (Figure 4). To remove surfactants in SWNTs, additional cleaning procedure was adopted to the buckypaper production process above. After, SWNT solution was vacuum filtered through a PTFE filter and stabilized for 15 minutes, the felt was rinsed twice with 250 ml of deionized water and 50 ml of acetone. The felt rinsed was stabilized under vacuum for 15 minutes before delaminated from a filter membrane, and the buckypaper was dried on a clean glass surface. (Figure 5). The buckypaper cleaned with this procedure showed smoother surface and other fabrication processes (e.g., cleaning) will be examined further.



Figure 4 Arc discharge SWNT (a) Felt (b) Buckypaper front (c) Buckypaper back



Figure 5 Arc discharge SWNT Cleaned with Acetone (a) Felt (b) Buckypaper front and, (c) Buckypaper back.

# **Fabrication and characterization of SWNTs obtained through arc discharge (AD) and high-pressure carbon monoxide (HiPco) syntheses**

## **INTRODUCTION**

Passive sampling of volatile organic compounds (VOCs) followed by laboratory analysis either through chemical or thermal extraction has been accepted in the workplace because of the convenience and cost effectiveness and wearer acceptability of passive sampler over active sampling devices. <sup>(1-3)</sup> However, passive samplers are generally limited in capability for very low exposure situations or short duration sampling because of their higher limit of detection caused by the relatively slow sampling rate driven by diffusion. <sup>(4)</sup> Moreover, for industries seeking to demonstrate regulatory compliance, the long time lag between collecting samples and getting results back <sup>(5)</sup> and expensive laboratory analysis have been a burden. Recently, our group developed a novel analytical technique called photothermal desorption (PTD) which can improve the sensitivity of the analysis of passive samplers and help shorten the current exposure assessment procedure to improve workers' protection by faster turn-around-time for analytical results. <sup>(6)</sup> In PTD, a pulse of light thermally desorbs analyte collected on a sorbent which releases VOC. VOC can be directly measured with a photo-ionization detector (PID) or directed to a gas chromatograph (GC) for detailed analysis. However, further development of a new sorbent which will work efficiently with this new desorption technique is still needed.

In this study, single-walled carbon nanotubes (SWNTs) were evaluated as potential sorbents for PTD because of their efficient light absorption <sup>(7,8)</sup>, exceptionally high thermal conductivity <sup>(9,10)</sup> and high Brunauer, Emmett, and Teller (BET) specific surface area <sup>(11)</sup>. While in general carbon nanotubes (CNTs) have shown promising features for VOC adsorption <sup>(12-14)</sup>, for passive sampling applications they need to be fabricated into a reusable, sturdy form which will preserve its physical integrity under normal working conditions. The purpose of this study was to examine fabrication methods of SWNTs to obtain BPs that are favorable for use with PTD. To accomplish this we compared their adsorption properties through examining BET surface area, average pore size, and toluene adsorption capacity. Previously, SWNTs synthesized by chemical vapor deposition (CVD) were examined due to their low cost and the scalability of synthesis. <sup>(6)</sup> However, we were unsuccessful in processing CVD SWNT into a self-supporting form (i.e., buckypaper, BP). Therefore, in this study SWNTs obtained through arc discharge (AD) and high-pressure carbon monoxide (HiPco) syntheses were investigated since we were able to easily process these into BPs in our lab.

High purity arc discharge (AD) SWNT and HiPco SWNT were purchased from NanoIntegris Inc (Quebec, Canada). AD SWNT (94.5 %) was pre-suspended in a surfactant solution (0.5 mg/mL, 1 % w/v sodium cholate and 1 % w/v sodium dodecyl sulfate in water). HiPco SWNT was powder (85 % pure). Vacuum filtration of liquid suspended SWNT was employed to fabricate BPs<sup>(15, 16)</sup> with a cleaning process added to remove potential surfactants from the AD SWNTs based on the manufacturer's recommendations<sup>(17)</sup>. For the fabrication of AD BPs, 100 mL (50 mg) of the AD SWNT suspension was mixed with 400 mL of acetone for 15 hours (Figure 1). The suspension was then vacuum-filtered through a polytetrafluoroethylene (PTFE) membrane filter (47 mm diameter, 5  $\mu$ m pore, EMD Millipore, Darmstadt, Germany) and allowed to dry for approximately 2 hours while on the filter membrane. A BP was obtained by delaminating the dried SWNT cake from the filter (non-cleaned AD BP). For solvent cleaned BPs, A series of two alternating rinses were used, a water rinse then solvent rinse was administered after the SWNT cake was deposited but not dried. The SWNT cake was first rinsed with 250 mL of deionized water (18.2 M $\Omega$ -cm) then 50 mL of solvent to make either acetone-cleaned or methanol-cleaned AD BP.



FIGURE 1. Typical fabrication procedure: CNT suspension - vacuum filtration - delamination (left to right)

For HiPco BP preparation, 50 mg of powdered HiPco SWNTs were suspended in 400 mL methanol and ultra-sonicated using a 490 W bath sonicator (BRANSON CPX5800H, Danbury, CT) for 90 minutes. The solution was vacuum-filtered through the same type PTFE membrane filter and allowed to dry for 30 minutes under vacuum plus another 2 hours without vacuum. The SWNT cake was then delaminated from the filter to obtain a BP (HiPco BP). Four BPs per each fabrication method were produced and each BP was investigated according to the diagram shown in Figure 2.

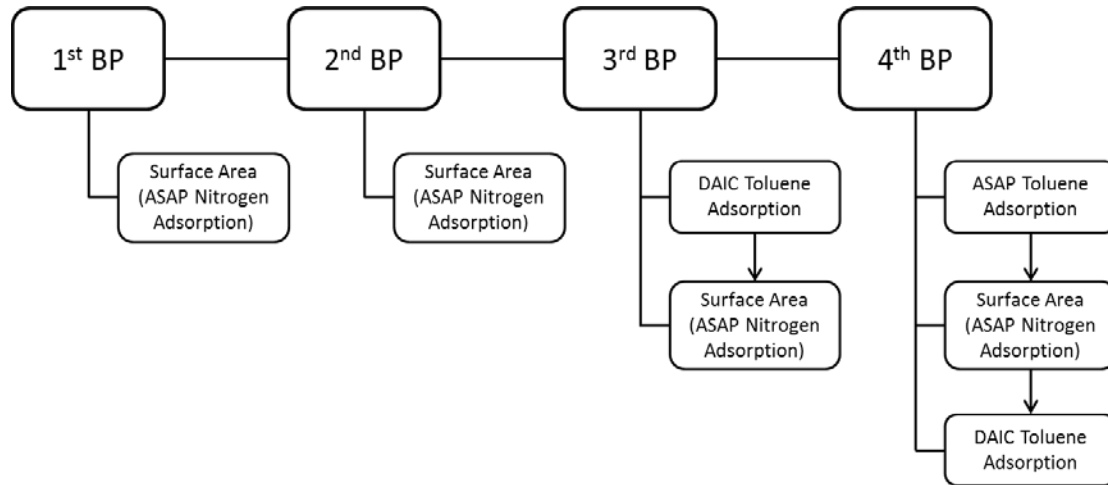


FIGURE 2. Diagram of measurements assigned to BPs per each fabrication method

#### Adsorption Characterization of BP

Three adsorption parameters were examined: BET surface area, average pore width, and toluene adsorption capacity. A physisorption analyzer (Micromeritics® ASAP 2020, Norcross, GA) was used to obtain surface area and average pore width by N<sub>2</sub> physisorption at 77 K. Samples were desorbed at 100 °C overnight in a lab oven prior to any adsorption parameter measurements. Degassing was conducted with the physisorption analyzer at 350 °C to further remove impurities prior analysis. Nitrogen adsorption isotherms were used to determine surface area by BET theory. The average pore width was determined using Equation (1):

$$d = \frac{4V}{A} \times 10^3 \quad (1)$$

Where:

d = average pore width (nm), assuming cylindrical pores

V = single point total pore volume (cm<sup>3</sup>/g) at relative pressure ≥ 0.995

A = surface area per unit mass of a sorbent determined by BET theory (m<sup>2</sup>/g)

Three BPs per fabrication method were analyzed by N<sub>2</sub> physisorption (Figure 2) with each sample analyzed in triplicate and results averaged.

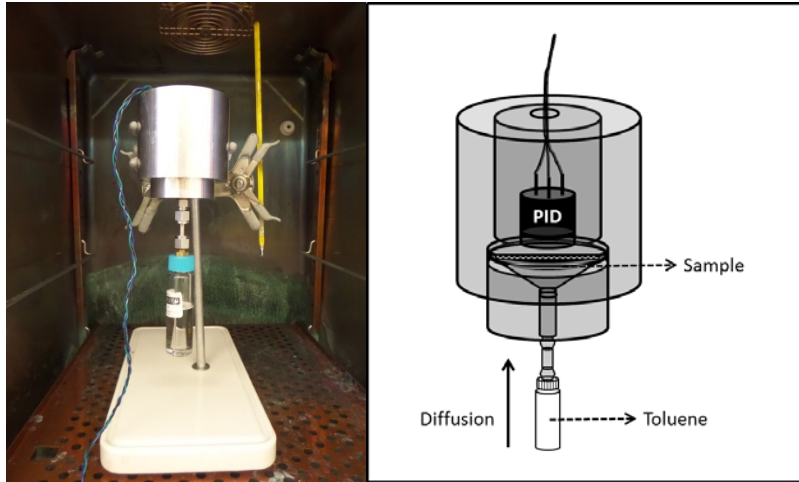


FIGURE 3. Diagram of Diffusive Adsorption Isotherm Chamber (DAIC) system

A diffusive based VOC adsorption isotherm chamber (DAIC) was designed in our lab to obtain toluene adsorption isotherms (30 °C, 303.15 K) and determine adsorption capacity at a given equilibrium concentration (Figure 3). Toluene flux into the DAIC system was first characterized with a toluene diffusion tube connected to an empty chamber. Toluene concentration in the chamber was continuously monitored with an embedded photo-ionization detector (PID, VOC-TRAQ, Baseline®, Lyons, CO). The mass flux of the toluene was determined by measuring the mass change in time as shown in Equations (2) and (3):

$$F = \sum_{i=1} \frac{\Delta m}{\Delta t} \quad (2)$$

Where:

F = mass flux of the adsorbate (µg/sec)

Δm = mass change of adsorbate in the chamber across the time interval (µg)

Δt = time interval between measurements (i.e., logging time interval of PID) (sec)

$$\Delta m = \left( \frac{\Delta C}{V_m} \times MW \right) \times V_c \times 10^3 \quad (3)$$

Where:

$\Delta C$  = concentration change of the adsorbate in the chamber during the time interval as measured with the embedded PID (ppm)

$V_m$  = 25.04; molar volume at the analytical temperature (303.15 K) and pressure (98992 Pa)

$MW$  = molecular weight of adsorbate (92.14 g/mol for toluene)

$V_c$ , = volume of the chamber ( $47.3 \times 10^{-6} \text{ m}^3$ )

The characterization measurements were repeated 6 times and a linear regression equation performed on all 6 trials to obtain an averaged adsorbate mass flux ( $R^2=0.85$ ) that accounted for the dynamic concentration gradient as the isotherm progressed (Equation 4):

$$F = -0.000158(C_{eq}) + 0.185214 \quad (4)$$

Where:

$F$  = mass flux of the adsorbate ( $\mu\text{g}/\text{sec}$ )

$C_{eq}$  = equilibrium concentration (ppm)

The mass adsorbed by a sorbent in a given isotherm was calculated using equation 4 from the time connected to the diffusion tube and the concentration in the DAIC. Adsorption was allowed to proceed until equilibrium concentration exceeded 800 ppm toluene. Adsorption capacity was expressed as mg (toluene)/ g (sorbent).

The third BPs from each fabrication method (Figure 2) was also analyzed for its toluene adsorption capacity using the DAIC system prior to surface area measurement.

To validate the DAIC system, activated carbon sorbent was placed in the DAIC and adsorption allowed to proceed for 2-18.5 hours with gravimetric confirmation of actual mass adsorbed at 5 time intervals (2, 2.3, 4, 5, 18.5 hours). The mean prediction was  $87.7 \pm 12.3 \%$  of actual mass.

Additionally two samples (one acetone-cleaned and one methanol-cleaned AD BPs) were sent to Micromeritics® for toluene adsorption analysis by ASAP 2020 physisorption analyzer. Samples were degassed for 960 minutes at 300 °C before analysis. Adsorption capacity was calculated by converting the adsorbate gas volume at STP (data obtained from the physisorption analysis) to toluene mass using Equations (5):

$$m_{adsorbed} = \frac{V_{Gas-STP} \times P_{STP} \times MW \times 10^3}{R \times T_{STP}} \quad (5)$$

Where:

$m_{adsorbed}$  = mass adsorbed per gram of sorbent (mg/g)

$V_{Gas-STP}$  = gas volume at STP obtained from the physisorption analysis (cm<sup>3</sup>/g)

$P_{STP}$  = standard pressure (101,325 Pa)

$MW$  = molecular weight of toluene (92.14 g/mol)

$R$  = ideal gas constant (8.314 Pa·m<sup>3</sup>/mol·K)

$T_{STP}$  = standard temperature (273.15 K)

After the samples were returned, toluene adsorption and BET surface area were re-analyzed since Micromeritics conducted a substantially longer degassing time (300 °C, 960 minutes) than was used in our lab (300 °C, 60 minutes).

## Results

### BET Surface Area & Pore Size

The BET surface area and mean pore diameter are as follows for non-cleaned AD, acetone-cleaned AD, methanol-cleaned AD, and HiPco BPs; 211 ± 61 m<sup>2</sup>/g (8.2 ± 0.1 nm), 322 ± 38 m<sup>2</sup>/g (9.7 ± 0.5 nm), 387 ± 16 m<sup>2</sup>/g (8.8 ± 0.4 nm), and 649 ± 3 m<sup>2</sup>/g (7.7 ± 0.3 nm), respectively (Table I). After degassing for 960 minutes at 300 °C, BET surface area and mean pore diameter were as follows; 205 ± 1 m<sup>2</sup>/g (9.7 ± 0.1 nm), 349 ± 10 m<sup>2</sup>/g (9.8 ± 0.1 nm), 421 ± 6 m<sup>2</sup>/g (8.6 ±

0.1 nm), and  $611 \pm 56 \text{ m}^2/\text{g}$  ( $7.3 \pm 0.3 \text{ nm}$ ) for non-cleaned AD, acetone-cleaned AD, methanol-cleaned AD, and HiPco BPs, respectively.

TABLE I. Surface area (SA) and pore size (d) analysis

Fabrication Methods		No long degassing		After 960 min degassing	
		SA ( $\text{m}^2/\text{g}$ )	d (nm)	SA ( $\text{m}^2/\text{g}$ )	d (nm)
AD BP	Non-cleaned	$211 \pm 61$	$8.2 \pm 0.1$	$205 \pm 1$	$9.7 \pm 0.1$
	Acetone-cleaned	$322 \pm 38$	$9.7 \pm 0.5$	$349 \pm 10$	$9.8 \pm 0.1$
	Methanol-cleaned	$387 \pm 16$	$8.8 \pm 0.4$	$421 \pm 6$	$8.6 \pm 0.1$
HiPco BP		$649 \pm 3$	$7.7 \pm 0.3$	$611 \pm 56$	$7.3 \pm 0.3$

In general, adsorption capacity is considered to be proportional to the surface area <sup>(18)</sup> while pore size distribution along with other parameters (e.g., characteristics of the adsorbates) also plays important roles in adsorption capacity. <sup>(19)</sup> Overall, HiPco BP had the highest surface area and the smallest pore diameter of the BPs fabricated, regardless of degassing. Among AD BPs, methanol-cleaned BPs had the highest surface area with minimal difference in the average pore width. A long degassing process improved surface area for acetone-cleaned and methanol-cleaned AD BPs while non-cleaned AD BPs and HiPco BPs show no improvement. For HiPco SWNTs which did not contain surfactants the degassing process did not show improvement. The cleaning process as well as the extended degassing of the AD CNTs helped remove some impurities and using methanol resulted in more adsorptive material than using acetone. Cinke et al. reported  $567 \text{ m}^2/\text{g}$  surface area with  $7.4 \text{ nm}$  average pore diameter of HiPco SWNTs (22 wt % as Fe) and a high increased surface area to  $1587 \text{ m}^2/\text{g}$  with decreased average pore width ( $3.9 \text{ nm}$ ) after two step purification process consisting of dimethylformamide/ethylene diamine treatment (first step) and HCl treatment and wet air oxidation at  $225 \text{ }^\circ\text{C}$  for 18 hr (second step). <sup>(20)</sup> Yang et al. obtained  $524 \text{ m}^2/\text{g}$  surface area ( $3.5 \text{ nm}$  average pore diameter) with HiPco SWNTs and observed an increased surface area of  $861 \text{ m}^2/\text{g}$  after air oxidation at  $350 \text{ }^\circ\text{C}$  for 30 min followed by HCl washing. <sup>(21)</sup> With an additional annealing at  $600 \text{ }^\circ\text{C}$  after HF treatment, the surface area of HiPco SWNTs was measured as high as  $1555 \text{ m}^2/\text{g}$ . <sup>(22)</sup> Raw AD SWNTs were measured to have  $376 \text{ m}^2/\text{g}$  and HCl treatment increased it to  $483 \text{ m}^2/\text{g}$ . <sup>(23)</sup> However, few data

on surface area of packed/ bundled form of CNTs such as BP has been reported in the literature.

As described above, differences in the surface area of CNT powders are often found. CNT are broadly categorized into SWNTs and multi-walled carbon nanotubes (MWNTs) <sup>(24)</sup> and also depending on the synthesis method each can be further categorized (e.g., CVD, AD, laser ablation, HiPco (only producing SWNTs)) <sup>(24-26)</sup>, which makes a difference in their physical and chemical properties. The exact type of CNT is not always available in the literature, different forms of CNTs (e.g., powder, solution, BP, etc.) are used, and a variety of solvents for cleaning are also available. Because of these circumstances there has not been an agreement on the magnitude of the surface area for each type of CNTs. In this study, we sought to determine which SWNT BP, AD or HiPco, has better adsorption properties, but our AD SWNTs were already suspended using surfactant in water which could have also contributed to the difference in this study. SWNTs in general are available in a variety of purity levels, but the same purity level is not always available in different types of SWNT. Most purification processes modify the physical and chemical properties of SWNTs by introducing defects in the tube walls and adding functional groups such as –COOH or –OH to the defects and tube ends. <sup>(27)</sup>. Our approach in this study was to maintain the physical/ chemical integrity of the SWNT substrates as much as possible by not challenging them with harsh conditions such as high temperature peroxide or acid digestion. We found that suspending CNTs in surfactants can negatively affect the BET surface area which can be corrected to varying degrees with solvent cleaning or extended degassing.

#### Toluene Adsorption Capacity

Toluene adsorption isotherms obtained with the DAIC system are shown in Figure 4. Adsorption capacities were determined at 800 ppm equilibrium concentration and found to be 25, 34, 46 and 106 mg toluene/ g BP for non-cleaned AD, acetone-cleaned AD, methanol-cleaned AD and HiPco BPs, respectively. The two samples sent to Micromeritics for verification of DAIC performance (acetone-cleaned and methanol-cleaned AD BPs) were degassed for a much longer time than was our practice (960 min vs 60 min) and were found to have much greater toluene adsorption capacity, 644 and 775 mg/g, respectively. When these same samples were re-measured using the DAIC system we found adsorption capacities to be 443 and 518 mg/g at 800 ppm for acetone-cleaned and methanol-cleaned AD BPs, respectively (Figure 4).

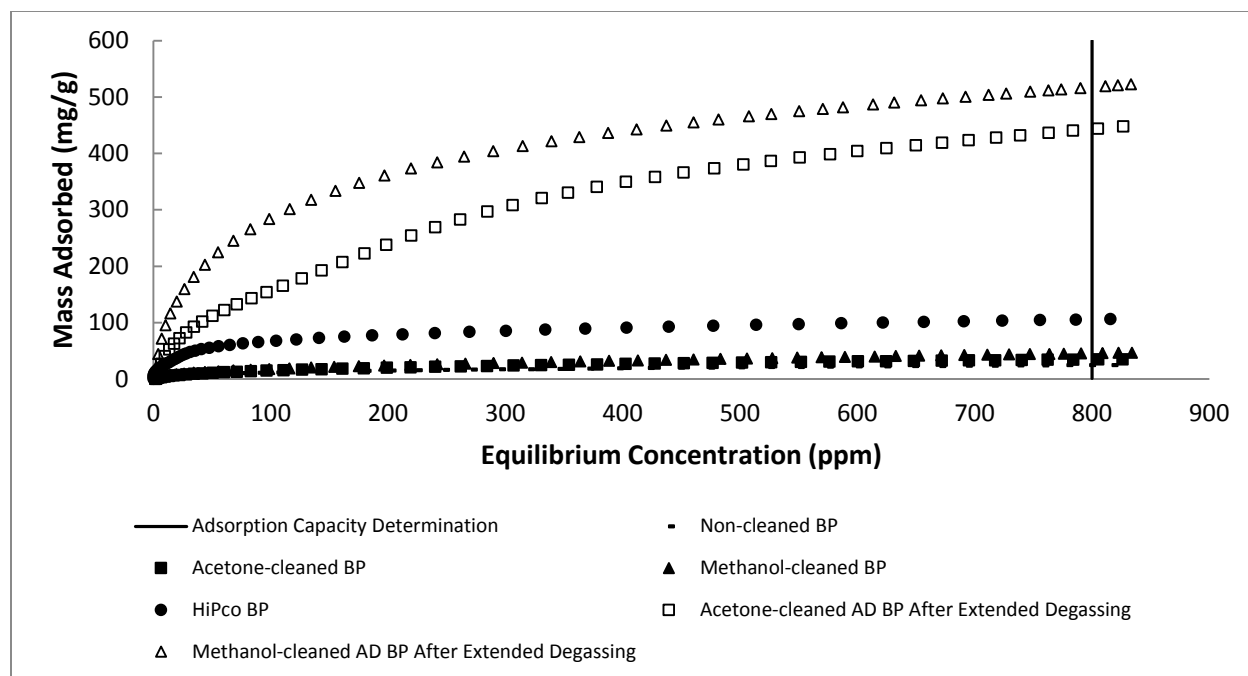


FIGURE 4. DAIC Isotherms

The toluene adsorption capacities obtained through our DAIC system and the physisorption analyzer were overall similar to each other with difference likely due to two major differences in experimental conditions. Adsorption capacities from the physisorption analyzer were at an equilibrium concentration of 28500 ppm at 25 °C while results from our DAIC system were from an equilibrium concentration of 800 ppm and 30 °C. At higher concentration and lower temperature adsorption capacity is expected to be larger, as was observed in these results.

Notwithstanding, higher toluene adsorption capacity was observed in materials with higher surface area. Adsorption capacities of the samples treated with extended degassing (300 °C for 960 min) showed greatly improved adsorption capacity (12-13 fold increase over solvent cleaning alone), but only modest increases in BET surface area.

CNTs have been extensively investigated for their adsorption for hydrogen storage [\(28-30\)](#) and more recently, literature has shown the use of CNTs in organic compound adsorption [\(14, 31, 32\)](#). Adsorption capacity of AD and HiPco SWNTs were examined with several VOCs and toluene was the greatest followed by methyl ethyl ketone (MEK), hexane, and cyclohexane for both types of SWNTs. [\(14\)](#) HiPco SWNTs exhibited higher adsorption capacity (average 356 mg/g) than AD SWNTs (average 216 mg/g) for all VOCs examined. Other organic compounds which have been tested include carbon tetrachloride (CCl<sub>4</sub>) with AD SWNTs [\(31\)](#) and hydrocarbons,

including ethanol, iso-propanol, cyclohexane, cyclohexene, benzene, and n-hexane, with SWNTs (not specified) (32). Adsorption of organic compounds as well as inorganics has often been performed in solution, mostly for water treatment applications. (33, 34) Further experiments on the adsorption and desorption characteristics of CNTs using other organic compounds need to be further explored.

## CONCLUSIONS

The solvent cleaning process increased BET surface area and decreased average pore diameter for AD BPs. We have observed that the extended high temperature degassing increased the surface area and toluene adsorption capacity of AD BPs, suggesting that the cleaning process did not completely remove surfactant residues. Adsorption capacity increased with increasing surface area of BPs but toluene capacities were much more increased considering the relatively modest increase in surface area after extended degassing. AD BPs will need heat treatment to improve their adsorption properties. Overall, HiPco BP had the best adsorption properties (i.e., surface area, average pore width, and toluene adsorption capacity) as well as a simpler fabrication process compared with AD BPs, indicating suitability for VOC passive sampling and analysis by PTD.

## References

- 1 **Pristas, R.:** Passive badges for compliance monitoring internationally. *American Industrial Hygiene Association Journal* 55(9): 841 (1994).
- 2 **Shih-Wei, T., and S.S. Que Hee:** A new passive sampler for regulated workplace ketones. *AIHAJ* 61(6): 808-814 (2000).
- 3 **Williams, C.E., P.N. Pintauro, and R.J. Rando:** A transient model of mass transfer and kinetics in a passive vapor sampler. *American Industrial Hygiene Association Journal* 56(11): 1074-1082 (1995).
- 4 **Berlin, A., R.H. Brown, K. Lechnitz, B. Miller, K.J. Saunders, and B. Striefler:** Diffusive Sampling—An Alternative Approach. *Applied Industrial Hygiene* 3(2): R-2-R-6 (1988).
- 5 **William F. Martin, J.M.L., Timothy G. Prothero:** *Hazardous Waste Handbook for Health and Safety*. Butterworth Publishers, 1987.

- 6 **Floyd, E.L., K. Sapag, J. Oh, and C.T. Lungu:** Photothermal desorption of single-walled carbon nanotubes and coconut shell-activated carbons using a continuous light source for application in air sampling. *Annals of Occupational Hygiene* 58(7): 877-888 (2014).
- 7 **Ajayan, P.M., M. Terrones, A. De la Guardia, V. Huc, N. Grobert, B.Q. Wei et al.:** Nanotubes in a flash - Ignition and reconstruction. *Science* 296(5568): 705 (2002).
- 8 **Mizuno, K., J. Ishii, H. Kishida, Y. Hayamizu, S. Yasuda, D.N. Futaba et al.:** A black body absorber from vertically aligned single-walled carbon nanotubes. *Proceedings of the National Academy of Sciences of the United States of America* 106(15): 6044-6047 (2009).
- 9 **Pop, E., D. Mann, Q. Wang, K. Goodson, and H. Dai:** Thermal conductance of an individual single-wall carbon nanotube above room temperature. *Nano Letters* 6(1): 96-100 (2006).
- 10 **Volkov, A.N., and L.V. Zhigilei:** Heat conduction in carbon nanotube materials: Strong effect of intrinsic thermal conductivity of carbon nanotubes. *Applied Physics Letters* 101(4)(2012).
- 11 **Bacsa, R.R., C. Laurent, A. Peigney, W.S. Bacsa, T. Vaugien, and A. Rousset:** High specific surface area carbon nanotubes from catalytic chemical vapor deposition process. *Chemical Physics Letters* 323(5-6): 566-571 (2000).
- 12 **Sone, H., B. Fugetsu, T. Tsukada, and M. Endo:** Affinity-based elimination of aromatic VOCs by highly crystalline multi-walled carbon nanotubes. *Talanta* 74(5): 1265-1270 (2008).
- 13 **Jahangiri, M., S.J. Shahtaheri, J. Adl, A. Rashidi, H. Kakoei, A.R. Forushani et al.:** The adsorption of benzene, toluene and xylenes (BTX) on the carbon nanostructures: The study of different parameters. *Fresenius Environmental Bulletin* 20(4 A): 1036-1045 (2011).
- 14 **Agnihotri, S., M.J. Rood, and M. Rostam-Abadi:** Adsorption equilibrium of organic vapors on single-walled carbon nanotubes. *Carbon* 43(11): 2379-2388 (2005).
- 15 **Shi, Z., X. Chen, X. Wang, T. Zhang, and J. Jin:** Fabrication of superstrong ultrathin free-standing single-walled carbon nanotube films via a wet process. *Advanced Functional Materials* 21(22): 4358-4363 (2011).
- 16 **Wu, Z., Z. Chen, X. Du, J.M. Logan, J. Sippel, M. Nikolou et al.:** Transparent, conductive carbon nanotube films. *Science* 305(5688): 1273-1276 (2004).

- 17 **NanoIntegris:** "How to Create CNT Thin Films with NanoIntegris CNTs in Aqueous Solution " [Online] Available at <http://www.nanointegris.com/en/downloads>
- 18 **Demiral, H., T. Demiral, B. Karabacakoğlu, and F. Tümsek:** Production of activated carbon from olive bagasse by physical activation. *Chemical Engineering Research and Design* 89(2): 206-213 (2011).
- 19 **Dobre, T., O.C. Paîrvulescu, G. Iavorschi, M. Stroescu, and A. Stoica:** Volatile organic compounds removal from gas streams by adsorption onto activated carbon. *Industrial and Engineering Chemistry Research* 53(9): 3622-3628 (2014).
- 20 **Cinke, M., J. Li, B. Chen, A. Cassell, L. Delzeit, J. Han et al.:** Pore structure of raw and purified HiPco single-walled carbon nanotubes. *Chemical Physics Letters* 365(1-2): 69-74 (2002).
- 21 **Yang, C.M., K. Kaneko, M. Yudasaka, and S. Iijima:** Effect of Purification on Pore Structure of HiPco Single-Walled Carbon Nanotube Aggregates. *Nano Letters* 2(4): 385-388 (2002).
- 22 **Lafi, L., D. Cossement, and R. Chahine:** Raman spectroscopy and nitrogen vapour adsorption for the study of structural changes during purification of single-wall carbon nanotubes. *Carbon* 43(7): 1347-1357 (2005).
- 23 **Eswaramoorthy, M., R. Sen, and C.N.R. Rao:** A study of micropores in single-walled carbon nanotubes by the adsorption of gases and vapors. *Chemical Physics Letters* 304(3-4): 207-210 (1999).
- 24 **Aqel, A., K.M.M.A. El-Nour, R.A.A. Ammar, and A. Al-Warthan:** Carbon nanotubes, science and technology part (I) structure, synthesis and characterisation. *Arabian Journal of Chemistry* 5(1): 1-23 (2012).
- 25 **M. M. A. Rafique, J.I.:** Production of Carbon Nanotubes by Different Routes - A Review. *J. of Encapsulation and Adsorption Sciences* (1): 29-34 (2011).
- 26 **Dai, H.:** Carbon nanotubes: Opportunities and challenges. *Surface Science* 500(1-3): 218-241 (2002).

- 27 **Itkis, M.E., D.E. Perea, S. Niyogi, S.M. Rickard, M.A. Hamon, H. Hu et al.:** Purity evaluation of as-prepared single-walled carbon nanotube soot by use of solution-phase near-IR spectroscopy. *Nano Letters* 3(3): 309-314 (2003).
- 28 **Liu, C., Y.Y. Fan, M. Liu, H.T. Cong, H.M. Cheng, and M.S. Dresselhaus:** Hydrogen storage in single-walled carbon nanotubes at room temperature. *Science* 286(5442): 1127-1129 (1999).
- 29 **Dillon, A.C., K.M. Jones, T.A. Bekkedahl, C.H. Kiang, D.S. Bethune, and M.J. Heben:** Storage of hydrogen in single-walled carbon nanotubes. *Nature* 386(6623): 377-379 (1997).
- 30 **Ye, Y., C.C. Ahn, C. Witham, B. Fultz, J. Liu, A.G. Rinzler et al.:** Hydrogen adsorption and cohesive energy of single-walled carbon nanotubes. *Applied Physics Letters* 74(16): 2307-2309 (1999).
- 31 **Babaa, M.R., N. Dupont-Pavlovsky, E. McRae, and K. Masenelli-Varlot:** Physical adsorption of carbon tetrachloride on as-produced and on mechanically opened single walled carbon nanotubes. *Carbon* 42(8-9): 1549-1554 (2004).
- 32 **Bittner, E.W., M.R. Smith, and B.C. Bockrath:** Characterization of the surfaces of single-walled carbon nanotubes using alcohols and hydrocarbons: A pulse adsorption technique. *Carbon* 41(6): 1231-1239 (2003).
- 33 **Fagan, S.B., A.G. Souza Filho, J.O.G. Lima, J. Mendes Filho, O.P. Ferreira, I.O. Mazali et al.:** 1,2-Dichlorobenzene interacting with carbon nanotubes. *Nano Letters* 4(7): 1285-1288 (2004).
- 34 **Chen, W., L. Duan, and D. Zhu:** Adsorption of polar and nonpolar organic chemicals to carbon nanotubes. *Environmental Science and Technology* 41(24): 8295-8300 (2007).

## Fabrication of CSP substrates through Hydrothermal Carbonization (HTC)

A typical hydrothermal synthesis of HTC includes the heating an aqueous solution of precursor in the range of temperatures from 130 to 250 °C in a Parr Model 4592 stirred MicroReactor. The controllable stirring and heating rate are essential process parameters for the synthesis of HTC with narrow size distribution and low aggregation. The precursor solution is added in a Teflon-

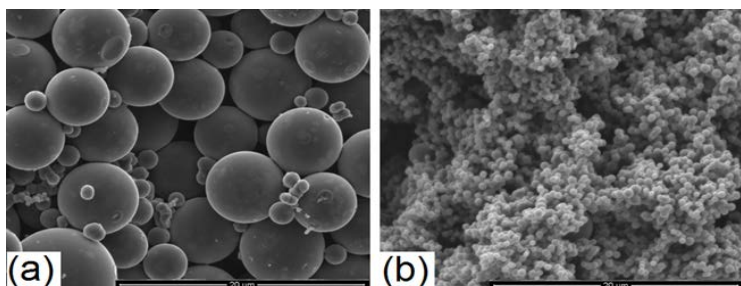


Figure 1. SEM images of HTC spheres a) microspheres with 420 m<sup>2</sup>/g porosity and (b) nanospheres with 550 m<sup>2</sup>/g. Average pore diameter was <1.5 nm in both cases.

lined autoclave, sealed, and kept at required temperature for certain periods of time (usually 4 – 12 hours). The concentration of the solution (0.1 – 0.5 M), process temperature and time, and the solution pH is optimized to reproducibly produce the planned shapes and sizes of model HTC.

Typical yield of carbonized material with a 50-ml pressure vessel ranges from 30 mg to 500 mg, depending on the precursor concentration and other process parameters (temperature, time, impurities, etc.). To increase the porosity of as-prepared HTC in the proposed study, the materials will be annealed in argon gas in the range of temperatures from 700 to 1000 °C. Chemical activation will be carried out by annealing the mixtures of HTC with KOH (typical hydroxide/HTC ratio of 2/1 by weight) at up to 750°C during 2 h under argon or nitrogen atmosphere. Following the activation procedure, the material will be washed sequentially with HCl and DI water and dried. Figure 1 shows SEM images of prepared microporous HTC without activator. We have established the reproducible experimental procedures in hydrothermal manufacturing of uniform spherical HTC with different dimensions in the range from 10 nm to 5 micrometers, surface morphology, chemical and phase composition, and surface functionalization. When annealed at 800 – 1000 °C without any activator, these materials showed 400 – 550 m<sup>2</sup>/g porosity and pore diameters below 1.3 nm.

Glucose, an inexpensive and abundant saccharide, was used as a precursor for the production of spherical HTC. Two concentrations of glucose were examined to fabricate carbonaceous spherical particles (CSPs); 0.5 g and 1.0 g. Each was dissolved in 10 mL DI water and 2.5 mL nickel ion (approximately 130 mg nickel dissolved in 50 mL DI water) and the solution was then transferred to an autoclave in which a Teflon liner was inserted, and the autoclave was placed into a furnace. Temperature was set at 170 °C with a ramping rate of 7 °C/min and soaking time

of 8 hours was followed. After the HTC process, the residual polymer solution was removed and about 10 mL of DI water was added to the remained colloid and then the solution was centrifuged (Fisher Scientific AccuSpin™ 400) for 10 minutes at 300 rpm. The cleaning process was repeated four times and colloid was dried at room temperature. With the higher concentration, around 130 mg of spheres were obtained while the lower concentration yielded less than a half of the amount generated in the higher concentration. Figure 2 shows scanning electron microscope (SEM) images of the CSPs obtained in the process. The low-concentrated CSPs were relatively mono-dispersed whereas the high-concentrated CSPs generated larger particles with poly-dispersed distribution.

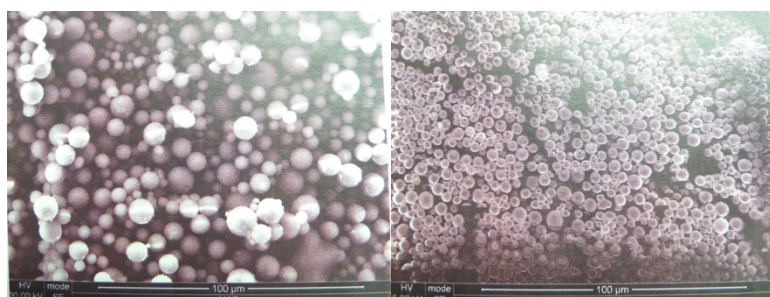


Figure 2. SEM images (a) CSPs (1 g glucose) and (b) CSPs (0.5 g glucose)

### Carbon nanofibers (CNF)

We have used electrospinning to fabricate CNF for various purposes, in particular, as a carrier substrate for microporous HTC spheres discussed above. It was found that by mixing PAN

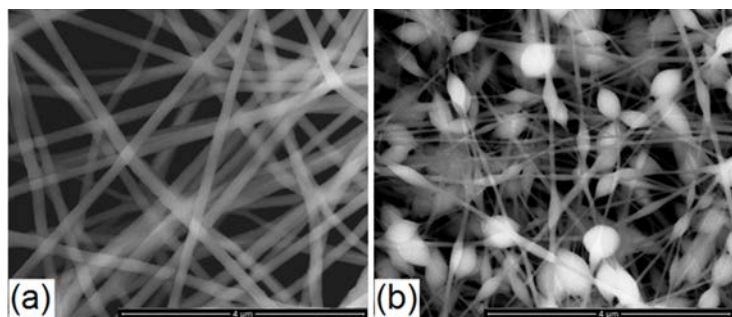


Figure 3. SEM images of electrospun PAN (a) and PAN/HTC (b) nanofibrous sheets. Scale bar is 4  $\mu$ m.

dissolved in DMF with dry HTC powder, it was possible to obtain up to 1:1 weight loading ration of PAN/HTC in the precursor and resulting fibers (Figure 3). In a typical experiment, a needle dc-electrospinning was utilized at 17 – 24 kV voltage with 6 – 10 wt% PAN in DMF and HTC spherical particles. It

can be seen if Fig. 3b that HTC particles are fully integrated into the PAN fibers, and PAN fibers maintained their continuity although their diameter reduced. However, it was difficult to prepare the PAN/HTC composite when the HTC particle size exceeded 0.5  $\mu$ m.

We started utilize a recently developed high-rate alternating current (AC) electrospinning

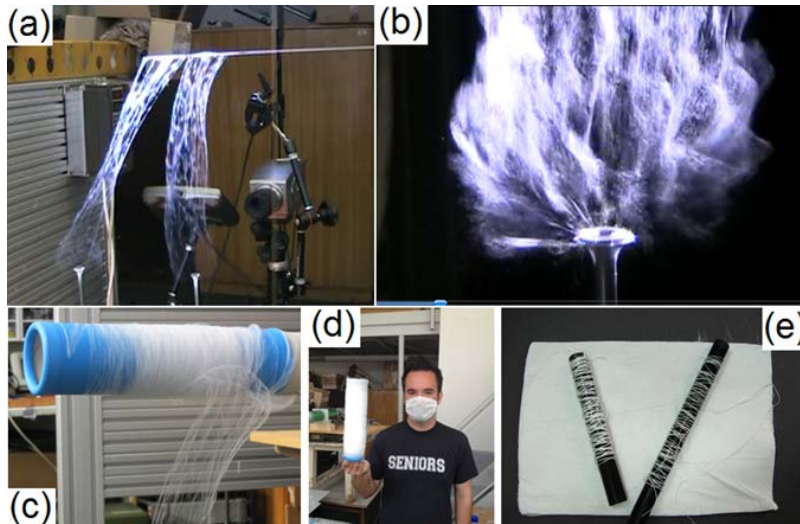


Figure 4. (a) Propagating binary fiber flows and (b) fiber jets generated in AC-electrospinning; (c) fiber flow is collected at up to 22 g/h rate (d); (e) Examples of ac-spun PAN nanofibrous sheet and yarn.

process to produce all nanofibrous materials combinations in this study. AC-electrospinning has been set up in Prof. Stanishevsky's laboratory in addition to the existing dc-electrospinning facilities. The AC-electrospinning introduces several new physical

phenomena into the process that led to significant reduction or elimination of major

disadvantages of dc-electrospinning such as “whipping” instability and residual fiber charge. AC-electrospinning offers much higher efficiency (up to 3 orders of magnitude) and flexibility in the generation and handling of nanofibers. The ac-field generated fibers are efficiently carried by corona wind without the need for an electrically grounded collector which makes easier the fiber collection and their shaping into the desired constructs. A number of polymer precursors for making fibers have been tested in this method. In the proposed study we will use AC-electrospinning with a two-electrode fiber generator as shown in Fig. 4. This will allow to generate two fiber flows simultaneously (Fig.4a), e.g. PAN and cellulose. In our preliminary ac-electrospinning experiments with PAN precursor at ac-voltages in the range 18–38 kV rms, the collected mass of nanofibers reached 15–22 gram/hour, which is more than 2 orders of magnitude larger when compared with a needle dc-electrospinning (0.05 – 0.2 gram/hour). Multiple polymer jets are generated from the electrode surface in this method (Fig.4b) and form relatively slowly moving (0.3 – 0.7 m/s) dense wavy flow of fibers, which can be easily captured with any suitable nonconducting element e.g., moving cotton thread, paper sheet, or rotating plastic cylinder (Fig.4a,c,d) and then shaped into the desired form (Fig.4e). Based on the literature and our preliminary results we expect the CNF/HTC constructs will also maintain their properties after the annealing and activation. Thus, using this new rapid electrospinning method we will prepare, in timely manner and sufficient quantities, the fibrous precursor sheets that will

allow the incorporation of HTC spherical particles and formation of self-supporting adsorbent pads.

## Co-I Dr. Evan Floyd's report

### University of Oklahoma Health Science Center

The key achievements of this subcontract are as follows:

- 1.) Developed a technique for fabricating HiPco buckypaper using a powdered nanomaterial source material.
- 2.) Developed a technique for recycling broken or failed buckypaper substrates.
- 3.) Developed a technique for mounting sorbent substrates to solid surfaces such as a glass window for easy sample handling, light irradiation and fast response surface mount thermocouple temperature measurement.
- 4.) Designed, specify and prototype a custom adsorption isotherm unit capable of automatic rapid materials characterization. Characterize the unit, implement and verify its performance, build 2 more and train collaborators on its use and implementation. Currently pursuing patentability.
- 5.) Conducted detailed adsorption characterization of HiPco buckypapers using toluene and acetone and the system described above.
- 6.) Designed and specify the capability, operation and form factor of a custom flash unit suitable for high performance photothermal desorption.
- 7.) Designed and prototype a photothermal desorption test unit that utilizes the sorbent substrates laminated to a glass window that can easily be incorporated into a diffusive sampler and handled by a technician repeatedly.
- 8.) Trained 3 students in this field, provide partial support for 2 master students, improved infrastructure for this line of work and strengthened inter-institutional collaboration between OUHSC and UAB.

In order to accelerate our ability to evaluate the photothermal response of the substrates that would be fabricated in this study I built upon my previous experience dispersing chemical vapor deposition (CVD) single walled carbon nanotubes (SWNT) in solvents. Previously I have found that stable suspensions (>1 year) could be achieved with the correct solvent (1,2-dichlorobenzene) and high energy sonication (450W, 70%) for approximately 90 minutes. From

this experience I also learned that this resulted in nearly mono-dispersed SWNTs which caused a very slow filtration (~6 hours) due to pore clogging and near penetration of the pores in the PTFE membrane filters used to collect the dispersed SWNT. While this dispersion technique resulted in a very flexible and durable buckypaper, it was not possible to separate the buckypaper from the membrane filter due to the penetration of SWNT into the pores of the membrane filter, and complete removal of 1,2-dichlorobenzene from the sorbent was not easy. Since we wished to maintain the least contaminated sorbent as possible, we did not switch to a different membrane filter that could be dissolved from the buckypaper (such as mixed cellulose ester dissolved with acetone) since this would inevitably result in contamination of the buckypaper with dissolved membrane polymers.

The development of a dispersion and filtration technique that was both time efficient and produced suitable quality self-supporting buckypapers was of utmost importance. Ultimately we discovered that 50 mg of HiPco SWNT could be dispersed in 300 mL of methanol using a 450W probe sonicator set to 70% power for 50 minutes (this was adapted to 50 minutes in a 480W bath sonicator at UAB). These dispersions appeared homogenous for approximately 10 minutes then small clumps resembling seaweed or algae began to form, typically while filtration was progressing. As a side note: a similar phenomenon was observed with Arc Discharge SWNT that were purchased from NanoIntegris pre-dispersed with surfactant in water. When this suspension was mixed with acetone (according to the manufacturer's instructions) the dispersion began to destabilize and form similar looking agglomerates. During filtration the agglomerates deposited uniformly across the filter and smoothed out very nicely. HiPco SWNT dispersed in methanol as described above were found to form buckypapers that were separable from the PTFE membrane with some care taken not to tear the delicate buckypaper.

Once a technique was established that reliably produced self supporting buckypaper sorbents, we began developing a technique to recycle the failed or broken buckypapers. This was a similar approach as above; sonication in methanol followed by membrane filtration. The broken or failed buckypapers were placed in a relatively small volume of methanol (~250 mL) and sonicated as above until a somewhat consistent sludge was formed. Small volume aliquots of this sludge was then diluted and further dispersed in 300 mL of methanol for 50 minutes at 450W, 70% power. The adsorption capacity of these buckypapers were found to be approximately 2/3 that of buckypapers made directly from virgin powder.

With an established technique for fabricating buckypapers we then focused on developing a technique for mounting solid objects to the buckypaper or the buckypaper to solid objects. Ultimately we found that after depositing SWNT on a membrane filter, they could be pressed against a solid surface (while still wet) and allowed to dry. This creates a strong bond that is not released when simply wetted with a solvent as may occur during chemical extraction. While SWNT depositions were still wet, they were pressed against a 2 inch glass disk that was to serve as an irradiation window during sample analysis. This same technique was applied to the surface mount thermocouples necessary to measure fast response thermal rise when irradiated with high intensity photo flash.

A crude prototype of the flash unit necessary to complete the thermal response and photothermal desorption aspects of this project was developed as well as a detailed design specifications and form factor requirement. This was submitted to a developer who was unable to produce a working prototype, after this failed attempt to develop a suitable flash unit prototype we sought out a new developer who was ultimately able to meet most of the requirements of our design specifications with limitations on the maximum light energy delivered to the sample and the maximum frequency of flashing capable when at maximum flash energy. These setbacks forced us to focus our efforts in different directions while we waited for the developer to produce the flash unit. In this time we developed an automated system for conducting VOC adsorption isotherms and explored the effect of air oxidation on the BET surface area and toluene adsorption capacity of buckypapers.

The automated system for conducting VOC adsorption isotherms was born out of the necessity to evaluate the quality of many substrates when determining a suitable fabrication technique. The isotherm technique previously used was very tedious and labor intensive, requiring frequent manual injections for 14-30 hours depending on adsorption capacity and sample mass. These extended experiments were not high through put and required an analyst to attend regularly. I developed a diffusion based system that continuously doses the sorbent with VOC vapor from a diffusion tube and continuously monitors the equilibrium concentration of the sorbent headspace using an embedded photoionization detector (PID). This system was designed, fabricated, prototyped and validated by our lab with an automated data reduction system developed by one of my students. The average isotherm duration was reduced to 4-6 hours which is easily manageable in a single day and no longer requires an analyst attend continuously to make injections. This has facilitated rapid feedback on the effect of certain fabrication or purification techniques and 2 more units were produced, one of which was delivered to UAB along with an

instruction manual and detailed hands-on training by me to ensure proper set-up and implementation of the diffusive adsorption isotherm chamber (DAIC) system. Patentability of this invention is currently being explored through the OUHSC intellectual property department.

Using this DAIC, we were able to conduct detailed experiments comparing the adsorption properties of virgin HiPco buckypapers and recycled HiPco buckypapers. We explored the effect of air oxidation (annealing) at various temperatures and durations. Ultimately we found that recycled buckypaper possessed approximately 2/3 the adsorption capacity as virgin buckypaper. We are not sure why this is the case, but it shows tremendous potential for downstream recycling of these materials or continuous recycling of failed product instead of disposing as hazardous waste. Additionally, we found that air oxidation increased the adsorption capacity of both virgin and recycled buckypapers and that 60 minutes at 300C was the best compromise between energy consumption, time, sorbent burn off (loss) and total adsorption capacity. Toluene adsorption capacity increased modestly (~50%) while Acetone adsorption capacity increased notably ~300%. We believe this is due to the addition of polar active sites which is why we have used the term “air oxidation” over the term “annealing”.

While waiting for the flash unit to be developed we designed and developed a low volume desorption chamber that can be attached to a PID for single analyte evaluation or to a Gas Chromatograph inlet for multi-analyte analysis. This photothermal desorption chamber uses the sorbent mounted to a glass disk. The glass disk serves as the sealing surface for the top of the chamber and as the window for photo irradiation of samples. The internal dead volume of this chamber is approximately 6 mL and has 1/8<sup>th</sup> inch Teflon tubing that can be interfaced with a capillary column union or fed directly into a GC cryotrap inlet. With the dead volume being somewhat large (6 mL) compared to that of an auto-sampler inlet (1 mL), the chromatographic resolution may be somewhat hindered, however a cryo focusing inlet or low temperature oven start would easily resolve this minor deficiency until a very low dead volume unit can be developed.

During the course of these experiments I was able to incorporate 2 master students, each partially funded for this project and one undergraduate student. While I know student training was not an aim of this sub-award or primary award, it is always an added benefit when students are able to share in the project and gain some level of support. As a whole, this project has yielded many successes that have improved my infrastructure, strengthened my inter-

institutional collaboration with UAB (Dr. Claudiu Lungu in particular) and advanced the potential of photothermal desorption.

## List of publications

1. E Floyd, K Sapag, J Oh, CT Lungu\* Thermal Desorption of Toluene from Single-walled Carbon Nanotubes and Granular Activated Carbon under Continuous Light Irradiation. *Annals of Occupational Hygiene*, 58(7):877-888, 2014.
2. Jonghwa Oh, Evan Floyd, Claudiu T. Lungu: Fabrication of Single-walled Carbon Nanotube (SWNT) Sorbent for Volatile Organic Compounds (VOCs) Sampling. American Industrial Hygiene Conference and Exposition, San Antonio, TX, June, 2014.
3. Jonghwa Oh, Evan L. Floyd and Claudiu T. Lungu: Surface Area and Toluene Adsorption Capacity for Fabricated Single-Walled Carbon Nanotube (SWNT) Buckypaper. NanoBio Summit, University of Alabama, Tuscaloosa, AL October 23-24, 2014 -Third place in the graduate student poster competition.
4. Floyd, E. Lungu, CT: Estimating Integrated VOC Exposure in Near Real-Time. American Industrial Hygiene Conference and Exposition, San Antonio, TX, June, 2014.
5. Lungu, CT. Oh, J. Floyd, E: Photo Thermal Desorption of Toluene from Single Walled Carbon Nanotube Adsorbent Pads in Air Samplers, podium presentation at CIMTEC 2014, 6th Forum on New Materials, Montecatini Terme, Italy, June 15-19, 2014.
6. Jonghwa Oh, Evan Floyd, Claudiu T. Lungu: Toluene Adsorption Efficiency of Fabricated Single-walled Carbon Nanotube (SWCNT) Buckypaper. American Industrial Hygiene Conference and Exposition, Salt Lake City, May 30 – June 4, 2015 - Best poster in session award. Award of the Nanoparticles Technology Committee.
7. J. Oh, C. T. Lungu, E. Floyd: Fabrication of Single Walled Carbon Nanotube (SWNT) Sorbent for Volatile Organic Compounds (VOCs) Sampling. 10th IOHA International Scientific Conference. London, UK April 25-30, 2015.
8. Claudiu T. Lungu, Jonghwa Oh, Evan. L. Floyd: Adsorption Characterization of Fabricated Single Walled Carbon Nanotube (SWNT) Buckypapers for Volatile Organic Compound (VOC) Sampling. Podium presentation at the AIHC&e, Salt Lake City, June 1-5, 2015.

9. E. Floyd, OUHSC, Oklahoma City, OK; C. T. Lungu, J. Oh, M. Saina, UAB:  
Evaluation of Self-Supporting, Single-Walled Carbon Nanotube Bucky Paper  
Sorbents for the Application in Diffusive Sampling and Photothermal Desorption.  
Podium presentation at the AIHC&e, Salt Lake City, June 1-5, 2015.